Contents lists available at ScienceDirect

Science of the Total Environment

journal homepage: http://ees.elsevier.com

Drivers of dinoflagellate benthic cyst assemblages in the NW Patagonian Fjords System and its adjacent oceanic shelf, with a focus on harmful species

Camilo Rodríguez-Villegas [a,b,l], Matthew R. Lee [b], Pablo Salgado [c], Rosa I. Figueroa [d], Ángela Baldrich [a,b,l], Iván Pérez-Santos [b,e], Stephen J. Tomasetti [f], Edwin Niklitschek [b], Manuel Díaz [g], Gonzalo Álvarez [h,i], Sandra L. Marín [j], Miriam Seguel [k], Laura Farías [l], Patricio A. Díaz [b,m,*]

[a] Programa de Doctorado en Ciencias, Mención Conservación y Manejo de Recursos Naturales, Universidad de Los Lagos, Camino Chinquihue Km 6, Puerto Montt, Chile
[b] Centro i~mar, Universidad de Los Lagos, Casilla 557, Puerto Montt, Chile
[c] Centro de Estudios de Algas Nocivas (CREAN), Instituto de Fomento Pesquero (IFOP), Enrique Abello 0552, Punta Arenas, Chile
[d] Centro Oceanográfico de Vigo, Instituto Español de Oceanografía (IEO), Subida a Radio Faro 50, 36390 Vigo, Spain
[e] Centro de Investigación Oceanográfica COPAS Sur-Austral, Universidad de Concepción, Campus Concepción, Concepción, Chile
[f] School of Marine and Atmospheric Sciences, Stony Brook University, Southampton, NY, USA
[g] Programa de Investigación Pesquera, Instituto de Acuicultura, Universidad Austral de Chile, Puerto Montt, Chile
[h] Facultad de Ciencias del Mar, Departamento de Acuicultura, Universidad Católica del Norte, Coquimbo, Chile
[i] Centro de Investigación y Desarrollo Tecnológico en Algas (CIDTA), Facultad de Ciencias del Mar, Larrondo 1281, Universidad Católica del Norte, Coquimbo, Chile
[j] Instituto de Acuicultura, Universidad Austral de Chile, Puerto Montt, Chile
[k] Centro Regional de Análisis de Recursos y Medio Ambiente (CERAM), Universidad Austral de Chile, Puerto Montt, Chile
[l] Department of Oceanography, Millennium Institute for Coastal Social Ecology (SECOS) and Center for Climate Research and Resilience (CR2), University of Concepción, Concepción, Chile
[m] CeBiB, Universidad de Los Lagos, Puerto Montt, Chile

ARTICLE INFO

Article history:
Received 23 January 2021
Received in revised form 20 April 2021
Accepted 21 April 2021
Available online xxx
Editor: Lotfi Aleya

Keywords
Alexandrium catenella
Dinoflagellate resting cysts
Chilean Patagonia
Redox potential
Meiofauna

ABSTRACT

In recent decades, the alteration of coastal food webs (via aquaculture, fishing, and leisure activities), nutrient loading, and an expansion of monitoring programs have prompted an apparent worldwide rise in Harmful Algae Blooms (HABs). Over this time, a parallel increase in HABs has also been observed in the Chilean southern austral region (Patagonia fjords). HAB species like *Alexandrium catenella*—responsible for Paralytic Shellfish Poisoning (PSP)—are of great public concern due to their negative socioeconomic impacts and significant northward geographical range expansion. Many toxic dinoflagellate species (like *A. catenella*) produce benthic resting cysts, yet a holistic understanding of the physical-chemical and biological conditions influencing the distributions of cysts in this region is lacking. In this study, we measured a combination of hydrographic (temperature, salinity, and dissolved oxygen) and sediment physical-chemical properties (temperature, pH and redox potential), in addition to meiofaunal abundances –as sediment bioturbators and potential cyst predators– to determine the factors influencing dinoflagellate cyst distribution, with emphasis on *A. catenella* in and around a "hotspot" area of southern Chile. An analysis of similarities (ANOSIM) test revealed significant differences ($p < 0.011$) in cyst assemblages between the fjords and oceanic environments. Permutational Analysis of Variance (PERMANOVA) showed significant effects of sediment temperature and silt proportion in explaining differences in the cyst assemblages. A generalized linear model (GLM) indicated that sediment temperature, silt/sand, anoxic conditions, and low abundances of Harpacticoida —a meiofauna herbivore group and potential bioturbator— are associated with the higher resting cyst abundances of the harmful species *A. catenella*. The implications for *A. catenella* resting cysts dynamics is discussed, highlighting physical-chemical and biological interactions and their potential for PSP outbreak initiation.

1. Introduction

As one of the most significant groups of phytoplankton, dinoflagellates are essential contributors to freshwater and marine primary production (Bravo and Figueroa, 2014; Kremp et al., 2018). Given that many dinoflagellate species are responsible for Harmful Algal Blooms (HABs) that can negatively impact coastal resources, fisheries, and/or human health, it is crucial to establish a refined understanding of their ecology and life cycles (Azanza et al., 2018; Figueroa et al., 2018). It is well established that many dinoflagellate species produce benthic cysts (Dale, 1983) with dormancy/quiescence cycles as part of their life histories (Fischer et al., 2018). These dinoflagellate benthic cysts sink in marine sediment where they can remain viable for as long

* Corresponding author at: Centro i~mar & CeBiB, Universidad de Los Lagos, Casilla 557, Puerto Montt, Chile.
E-mail address: patricio.diaz@ulagos.cl (P.A. Díaz)

https://doi.org/10.1016/j.scitotenv.2021.147378
0048-9697/

as a century, enhancing the resistance of such species to adverse environmental conditions (Ribeiro et al., 2011; Ribeiro et al., 2013), as well as their geographical expansion, genetic variability, via the recombination of chromosomes, and the opportunistic use of favorable conditions by seeding bloom initiations (Anderson et al., 2005; Bravo and Figueroa, 2014; Brosnahan et al., 2017; Rodríguez-Villegas et al., 2020).

Over the last few decades, an apparent global expansion of HABs has been observed, associated in part with increasing anthropogenic pressure (e.g. aquaculture, nutrient loading, fishing, and leisure activities), and to the enhanced coverage and frequency of HAB monitoring programs (Anderson et al., 2008; Hallegraeff, 1993; Hallegraeff, 2010; Xu et al., 2019). Against this backdrop of global HAB expansion, a regional rise and apparent northward expansion of HABs has also been observed in Southern Chile, particularly, in the NW Patagonian Fjords System and adjacent oceanic areas (Díaz et al., 2019; Hernández et al., 2016), where HAB events have repeatedly caused severe negative socio-economic impacts (Díaz et al., 2014; Díaz et al., 2019; Guzmán et al., 1975; Guzmán et al., 2002; Molinet et al., 2003).

Species such as *Alexandrium catenella,* the saxitoxin producer and causal agent of Paralytic Shellfish Poisoning (PSP) (Guzmán et al., 2002), and yessotoxin producers, like *Protoceratium reticulatum*, *Lingulodinium polyedrum,* and *Gonyaulax spinifera* (Tubaro et al., 2010), produce dinoflagellate benthic resting cysts associated with HAB outbreaks in the NW Patagonian Fjords System and are a public concern due to the negative economic and human health outcomes that are associated with their blooms. Particularly for *A. catenella* outbreaks, a paradoxical pattern characterized by high seawater cell densities and acute toxicity despite the low densities of benthic cysts found in sediments, within the NW Patagonian Fjord System has been observed (Álvarez et al., 2019; Band-Schmidt et al., 2019; Díaz et al., 2014; Hernández et al., 2016; Molinet et al., 2003).

Two main hypotheses have been proposed to explain the previous paradox: i) *Alexandrium catenella* blooms in the NW Patagonian Fjord System develop from massive deep water circulation processes that favor re-suspension of benthic cysts stored in adjacent oceanic areas and transportation into the fjords (Mardones et al., 2016); and, alternatively, ii) the spatio-temporal variation in the *A. catenella* blooms is determined by the biological interactions (predation and/or bioturbation) between benthic cysts and meiofauna assemblages (Persson, 2000). Meiofaunal organisms (45–1000 μm) are a diverse and abundant component of the benthic ecosystem (Giere, 2009), where several species have been shown to predate on dinoflagellate benthic cysts (Franco et al., 2008; Pati et al., 1999). Meiofauna bioturbation may also affect dinoflagellate benthic cysts by transporting them deeper into anoxic conditions, away from potential consumers (Genovesi-Giunti et al., 2006; Persson, 2000). In both cases, the meiofauna (mainly Harpacticoida, Nematoda, and Foraminifera) could have a significant effect on the population dynamics of dinoflagellates (Pati et al., 1999). Neither of the previous two hypotheses has been tested so far, likely due to the strong focus on water column processes and physical-chemical variables that have characterized monitoring and research programs carried out in this area (Varela et al., 2012).

The distribution, composition, and abundance of HAB species can be obtained by benthic mapping of the cyst stages in surface sediments (Figueroa et al., 2018). The primary purpose of this mapping is to develop a biogeographic framework for the potential risk of HAB formation in susceptible areas. In this context, the germination process of dinoflagellate benthic cysts is crucial to species persistence, coupling planktonic/benthonic environments (Díaz et al., 2014; Figueroa et al., 2018). The limitation is that this process only occurs in response to a combination of favorable temperature, oxygen availability, and release from dormancy (Brosnahan et al., 2020; Genovesi-Giunti et al., 2006; Genovesi et al., 2009).

In this study, we assessed for the first time the potential relationship between dinoflagellate benthic cysts (abundance and species composition) and meiofauna assemblages in the NW Patagonian Fjords System and its adjacent oceanic shelf. We also assessed the potential of several physical-chemical measurements, collected in the water column and the sediment, to explain distribution patterns of dinoflagellate benthic cysts including among harmful species, such as *A. catenella* and *P. reticulatum*.

2. Material and methods

2.1. Study area

The NW Patagonian Fjords System, hereafter, NW Patagonian Fjords are formed by numerous channels, sounds, gulfs and fjords, which cover a geographical area of 100,000 km^2, from the Reloncaví Sound (41°S) in the north to the Taitao Peninsula (47°S) in the south (Iriarte et al., 2014; Silva and Vargas, 2014). The complexity characterizing this area derives from an intricate coastal morphology, an abrupt bathymetry, and the presence of several shallow constriction-sills, 0.5–10 km wide and 50–100 m deep, that restrict deep water flow (Fig. 1), such as the Desertores (−42.6°S) and the Meninea (−45.3°S) constrictions (Silva et al., 1995; Silva and Vargas, 2014).

The vertical structure of this area is formed by two main temperature and salinity layers (Pérez-Santos et al., 2014; Silva and Calvete, 2002). A warmer surface layer (5–10 m) characterized by variable salinity, the influence of freshwater inputs (rainfall, glacial melting, and rivers like Puelo, Petrohue, Cisnes, and Palena rivers), strong advection to and from channels, and wind- and tidal-driven vertical mixing (Pérez-Santos et al., 2014; Sievers and Silva, 2008; Silva et al., 1995), and a deeper layer (10–350 m) with more stable conditions.

Another relevant oceanographic aspect of the study area is the presence of distinct water masses that can be identified using salinity criteria (Sievers, 2008; Sievers and Silva, 2008). In the upper few meters of the water column Estuarine Waters (EW) are characteristic of this system; these can be sub-divided in Estuarine Fresh Water (EFW, salinity range: 11–21) and Estuarine Salty Water (ESW, salinity range: 21–31) (Pérez-Santos et al., 2014; Sievers and Silva, 2008). The mixing of EW with Subantarctic waters (SAAW, salinity range: 33–33.9) results in Modified Subantarctic water (MSAAW, salinity range: 31–33). Equatorial Subsurface Water (ESSW salinity range: >34) is also recognizable in this area (Pérez-Santos et al., 2014; Sievers and Silva, 2008).

No detailed studies about sediment characteristics are available for the Patagonian Fjords and its adjacent shelf. Nonetheless, a negative correlation between Total Organic Content (TOC) and particle size has been reported (Silva and Palma, 2006), following a zonal (east-west) gradient where TOC increases towards the heads of the fjords given the significant contributions of organic material made by the river systems (Aracena et al., 2011).

2.2. Field sampling

Recent sediments were sampled at 26 stations from the NW Patagonian Fjords and adjacent oceanic areas, during the CIMAR 24 cruise, onboard the Chilean Navy's research vessel AGS-61 *Cabo de Hornos* from 24 September to 18 October 2018 (austral spring). Of these 26 stations, 14 were designed to represent the NW Patagonian fjords, and 12 were designed to represent the adjacent oceanic area (Fig. 1). At each sampling station, water column temperature, salinity, and dissolved oxygen profiles were measured using a CTDO/Rosette probe

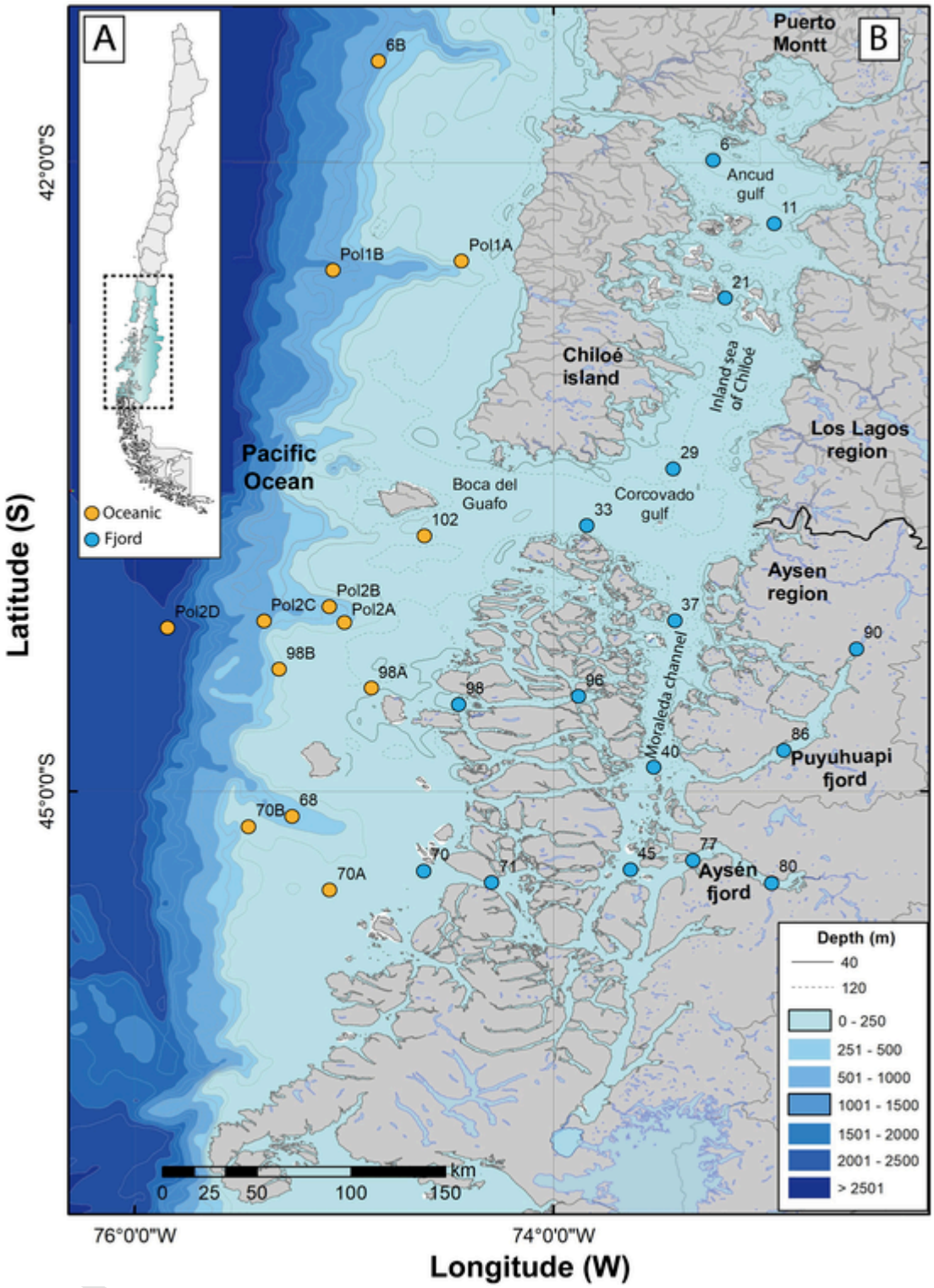

Fig. 1. Map showing: A) Chile (box delimited Los Lagos and Aysén regions); B) NW Patagonian Fjords System and its adjacent oceanic shelf showing the location of the sampling stations at the fjords (blue circles) and oceanic (orange circles) environments during the CIMAR 24 cruise. (For interpretation of the references to color in this figure legend, the reader is referred to the web version of this article.)

SeaBird 25-plus at a sampling rate of 8 Hz with a descent rate of 1 ms^{-1}, allowing a vertical resolution of 1 m.

Simultaneously, for inorganic nutrient analyses nitrates (NO_3^-), nitrites (NO_2^-), phosphates (PO_4^{3-}), and silicates (SiO_3^{2-}) surface water samples (5 m depth) were collected in triplicate 15 ml polyethylene flasks. The samples were filtered with 0.7 μm grade GF/F filters (Wat-man®) and stored in the darkness at −20 °C until the laboratory analysis. These analyses were performed according to colorimetric techniques described by (Grasshoff et al., 1983) through a Technicon Auto-Analyzer® (AA3 Seal Analytical). Ammonium (NH_4^+) was collected in triplicate 50 ml borosilicate glass flasks (previously aged with the working solution; (Holmes et al., 1999), which were filled until

20 ml with seawater obtained directly from Niskin bottle, plus working solution (5 ml) (Holmes et al., 1999). Immediately after 4 h (maintained in darkness and at 1–2 °C), each flask was incubated for 2 h at 40 °C. Then the absorbance was obtained by fluorometric measurement (Fluorometer Turner Design AquaFluor).

Sediment samples were collected at each station with a 0.1 m^2 Van Veen grab for further quantification of dinoflagellate benthic cysts and meiofauna, and granulometry analysis. Three sub-samples for dinoflagellate benthic cysts were obtained from the first 3 cm of the grab using a plastic corer of 8 cm length x 6 cm diameter. To avoid stimulating cyst germination by oxygen, light, and temperature changes, each sub-sample was manually released of air bubbles, wrapped in aluminum foil and preserved at 4 °C in the laboratory until analysis.

For meiofauna, five sediment sub-samples of 50 ml each were collected with a plastic syringe modified to form a piston corer and fixed in 5% formalin. For granulometry analysis, 500 cm^3 of sediment was collected and processed as described below.

Simultaneously, 3 to 9 records of temperature, pH, and redox potential (redox hereafter) were taken at random positions in each Van Veen grab from the sediment surface, using a pre-calibrated Multi-parameter portable MultiLine® meter (Multi 3620 IDS probe, WTW) with electrodes designed for measuring semisolids. For pH, records were collected with a conic electrode with Teflon, fiber, and ceramic triple-union, with temperature compensation. For redox determination we used a platinum sensor Ag/AgCl saturated (3.5 M KCL), with gel/polymer electrolyte. All measurements were made according to the Chilean standard ISO NCh: 17025 of 2005.

2.3. Sediment grain size composition

The sediment samples were freeze-dried and then analyzed using a series of sieves (500, 250, 150, 90, and 63 μm). Each sample was shaken for 15 min in a mechanical sieve shaker. The weight of the sediment fraction retained in each sieve and the pan (<63 μm) was then recorded. These data were then used to calculate the granulometry parameters using the rysgran package in R (De Camargo, 2016). The grain size composition of sediment was categorized using the Wentworth (1922) scale chart as follows: gravel ≥2000 μm, sand 63–2000 μm, and silt ≤63 μm. To summarize and characterize each sampling station, the three sediment subsamples from each station were averaged.

2.4. Sediment processing and cysts counting

Dinoflagellate cysts were extracted and identified to genus or species from all samples following the procedures outlined by Matsuoka and Fukuyo (2000), with slight modifications. Briefly, 3 cm^3 of sediment sample was suspended in 0.2 μm filtered seawater and sonicated (Labsonic 1000 l/Braun Sonic) for 1 min. Then, this suspension was washed through sieves of 106 μm and 20 μm mesh. The contents of the 20 μm sieve was then transferred to a Petri dish for cysts collection. The cysts were detached and suspended using filtered seawater and by swirling the plates. Heavy sediment particles remained at the center of the bottom of the dish, and the cysts remained in suspension in the circulating water. The resultant suspension volume was then transferred to a 50 ml glass graduated cylinder, and filtered seawater was added to achieve a final volume of 20 ml. Three 1 ml subsamples were analyzed using a Sedgewick-Rafter counting chamber with observations made using an inverted microscope with phase-contrast illumination (Olympus BX40). Only dinoflagellate cysts with intact cytoplasmic content were considered viable (Anderson et al., 1987; Genovesi-Giunti et al., 2006).

2.4.1. Meiofauna sample analyses

The meiofauna from each 50 ml sample was extracted using a two-stage methodology described by Lee et al. (2017). The fauna was removed from the substrate by decantation (Pfannkuche and Thiel, 1988), using 45 μm filtered fresh water. The extraction procedure was repeated five times. The material captured on the 45 μm sieve was then further processed using the Ludox flotation method (Burgess, 2001). This removes any remaining sediment from the sample. The samples were washed into 50 ml conical tubes with Ludox (a colloidal silica solution with a density of 1.15 g cm^{-3}). The samples were then centrifuged at 750 rpm for 15 min, after which the Ludox was poured slowly through a 45 μm sieve with care being taken not to re-suspend the sediment at the bottom of the tube.

The fauna extracted from the quantitative samples was then washed into embryo dishes with a glycerol solution (5% glycerol, 20% ethanol, and 75% distilled water) and placed in a warm desiccator for a period of between 24 and 48 h. Once the water and alcohol had evaporated, leaving the fauna in glycerol, the samples were mounted on large glass microscope slides (75 × 38 mm) within a wax ring. When the fauna was present in very high densities or when there was a significant amount of organic material in a sample, the sample was divided between two or more slides to facilitate analysis. The meiofauna present in each sample was assessed using an Olympus BX43 compound microscope. Each slide was systematically examined at a magnification of 100×, and the abundance of each taxonomic group was determined.

2.5. Data analysis

Non-metric multidimensional scaling (nMDS) based on the Bray–Curtis distance matrix (Legendre and Legendre, 1998) was employed to evaluate significant differences in the dinoflagellate cyst assemblages between the fjord and oceanic sites. Dimensionality was determined by a poorness-of-fit criterion (stress) calculated by calculating the square root of a normalized residual sum of squares. An ordination with stress of 0 to 0.05 provides an excellent representation or fit, but the stress of 0.3 is unacceptable for its poor representation (Clarke and Warwick, 1994). Analysis of similarities (ANOSIM) was applied to determine differences between sites. ANOSIM is widely used to test hypotheses about the spatial variations in assemblages (Clarke, 1993). The ANOSIM statistic R is based on the difference of mean ranks between and within groups. Similarity percentages and species contributions to the differences between sites were estimated using the similarity percentages (SIMPER) method.

A marginal Permutational Analysis of Variance (PERMANOVA) based on Bray-Curtis dissimilarities (Anderson, 2014; Paliy and Shankar, 2016) was carried out using "adonis2" function from the "vegan" package (Oksanen et al., 2018) to identify the influence of physical-chemical explanatory variables such as sediment Redox, pH, temperature, sand, silt, and biological variables such as Nematoda, Harpacticoida, and Foraminifera abundances over the resting cysts community. An empirical pseudo-*F*-statistic *p*-value in the model was calculated using 10.000 permutations (Oksanen et al., 2018).

A generalized linear model (GLM) with log-link function for negative binomial distribution (McCullagh and Nelder, 1989), was implemented to evaluate the influence of different environmental factors on the resting cysts abundances of the toxic dinoflagellate *Alexandrium catenella*, using as predictor variables sediment redox, temperature and pH, sand, silt, Nematode, Harpacticoida, and Foraminifera abundances. Previously, residuals homoscedasticity was tested by the Levene test, and the Collinearity between variables was checked by Variance Inflation Test (VIF) using a threshold ≤4 (Fox and Weisberg, 2011). As a result, gravel was removed to avoid collinearity with sand and silt variables. Finally, data overdispersion (OD) for the negative binomial

model was assessed by comparing observed and expected dispersion values (Crawley, 2007; Venables and Ripley, 2010).

Only main effects were included in the model as interactions between many variables might spuriously obscure their effects (Gotelli and Ellison, 2004). Explanatory variable effects were determined using a X^2marginal test type II ANOVA (Venables and Ripley, 2013).

All physical-chemical data were represented graphically using Ocean Data View with a surface view and applying diva gridding interpolation (Schlitzer, 2019), while statistical analyses were made using the statistical and programming software R 3.5.3 (R Core Team, 2019), "vegan","lme4" and "MASS" packages, available through the CRAN repository (http://www.r-project.org). Following recommendations from the American Statistical Association (Wasserstein and Lazar, 2016) and an increasing number of scientists worldwide (Amrhein et al., 2019), we avoid a dichotomic use of *p*-values, which are, instead, provided as calculated, except when summarizing several values into a single group.

3. Results

3.1. Hydrography and sediment physical-chemical conditions

The sea surface temperature (SST) showed a meridional pattern characterized by a gradient of warmer water (11 °C) in the north (42° S) and cooler (< 10 °C) in the south (45° S) of the study area (Fig. 2A). The warmer surface water passes through the Boca del Guafo and expands to the north (inland sea of Chiloé) and south (Moraleda Channel)

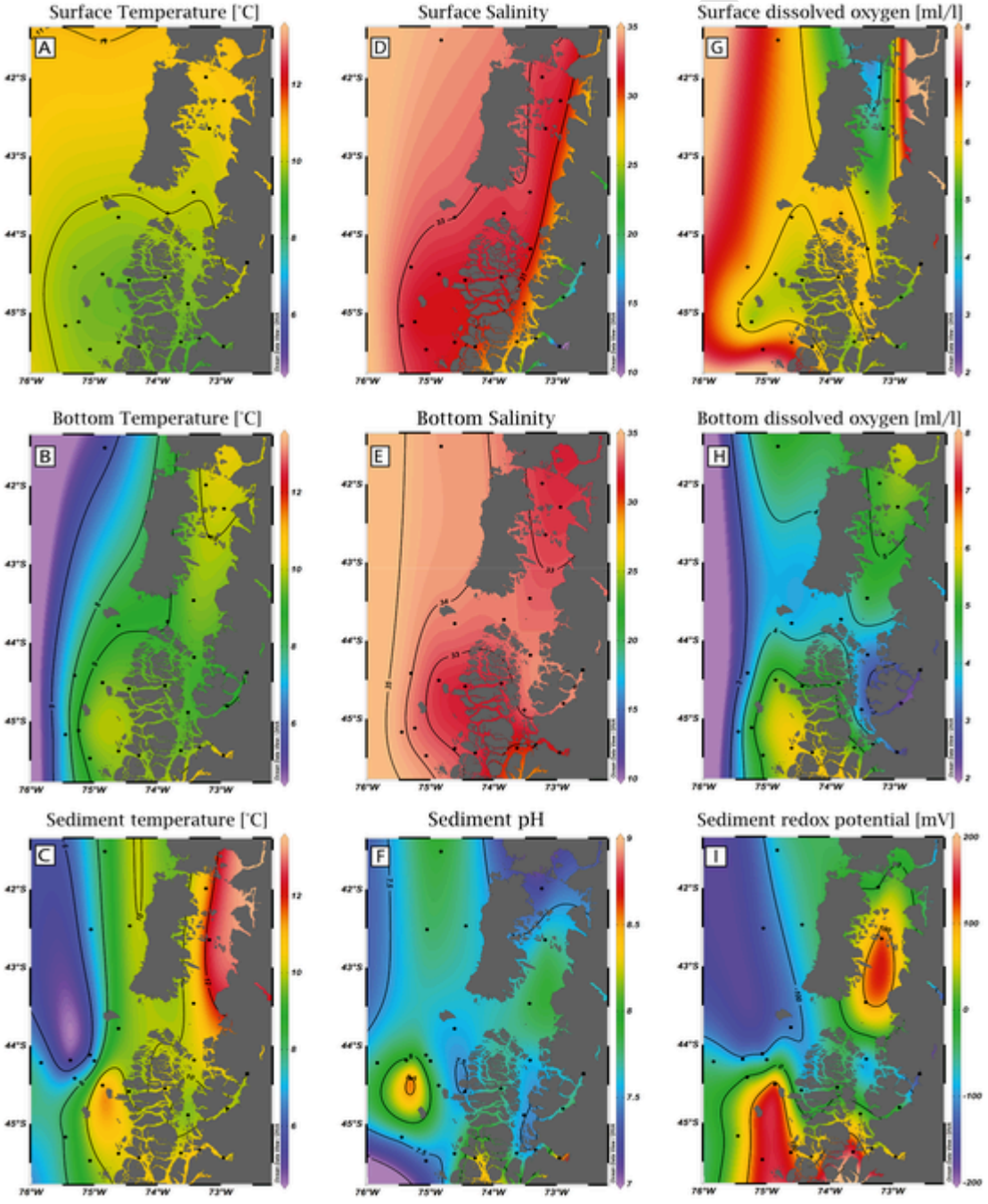

Fig. 2. Spatial variability of the water column and sediment physical-chemical parameters in the study area. A–C) Surface temperature (°C); bottom temperature (°C); and sediment temperature (°C); D–F) Surface salinity, bottom salinity, and sediment pH; G–I) Surface dissolved oxygen (ml/l), bottom dissolved oxygen (ml/l) and sediment Redox potential (mV).

of the study region (Fig. 2A). The highest bottom temperature (10.6 °C) was registered in the Ancud Gulf in the north of the inland sea of Chiloé (Fig. 2B). A zonal (west-east transect) bottom temperature gradient from the Pacific adjacent to the Aysén region to the Aysén Fjord with a range of 9.70 to 9.36 °C was also observed (Fig. 2B). In general, the bottom temperature maintained the same meridional pattern but temperatures were lower than surface temperatures (Fig. 2B). The sediment temperature was highest (~13 °C) in the inland sea of Chiloé (est. 21) an area with considerable oceanic influence (Fig. 2C). Sediments from the fjord and oceanic environments showed median values of 10.2 °C (IQR = 0.426) and 7.84 °C (IQR = 2.08) respectively (Fig. 3B).

A zonal gradient pattern was observed for surface salinity, with the lowest salinity (<31) within the fjords and channels, and higher salinities to the west in more oceanic waters (>31) (Fig. 2D). In the adjacent open ocean, the presence of MSAAW (31–33) and SAAW (>33) was observed (Fig. 2D). From north to south, the freshwater flow from the rivers Puelo (Reloncaví Fjord, 41.5°S), Palena (Pitipalena Fjord, 43.7°S), Cisnes (Puyuhuapi Fjord, 44.8°S), and Aysén (Aysén Fjord 45.3°S), resulted in lower salinities in the inland sea of Chiloé and the Moraleda Channel (Fig. 2D). The bottom salinity distribution showed clear associations with the water masses SAAW, ESSW, and the Antarctic Intermediate Water (AAIW, >34) (Fig. 2E).

The sediment pH values did not show a zonal and meridional distribution pattern (Fig. 2F). The lowest pH value (7.04) was registered at a sampling station located in the northern part of inland Chiloé sea (est. 6), while the highest values were observed in the Aysén Fjord at station 80 (8.52) and the oceanic shelf station 98 B (8.87) adjacent to the Aysén Fjord. Overall, sediments from the oceanic and fjord environments showed median pH values of 7.74 (IQR = 0.154), and 7.62 (IQR = 0.314) respectively (Fig. 3C).

Surface dissolved oxygen showed an irregular distribution pattern with values ranging from 5 ml l^{-1} to 8 ml l^{-1} (Fig. 2G). In bottom water samples, dissolved oxygen was very low, e.g., in Puyuhuapi and Aysén fjords the values were 2–3 ml l^{-1} (Fig. 2H).

The distribution of redox values in the sediment samples permitted the identification of 4 areas with specific characteristics: first, an oxygenated east-west zonal gradient from Aysén Fjord to the adjacent ocean. A second area with an anoxic east-west zonal gradient from Puyuhuapi Fjord to the adjacent ocean; the third area was oxygenated with a north-south meridional located in the inland sea of Chiloé, and the fourth area presented a predominant anoxic zonal and meridional gradient on the exterior continental shelf off Chiloé (Fig. 2I). Sediments from the oceanic and fjord environments showed median Redox values of −66.86 mV (IQR = 144.03) and 30.90 mV (IQR = 166.59) respectively (Fig. 3D).

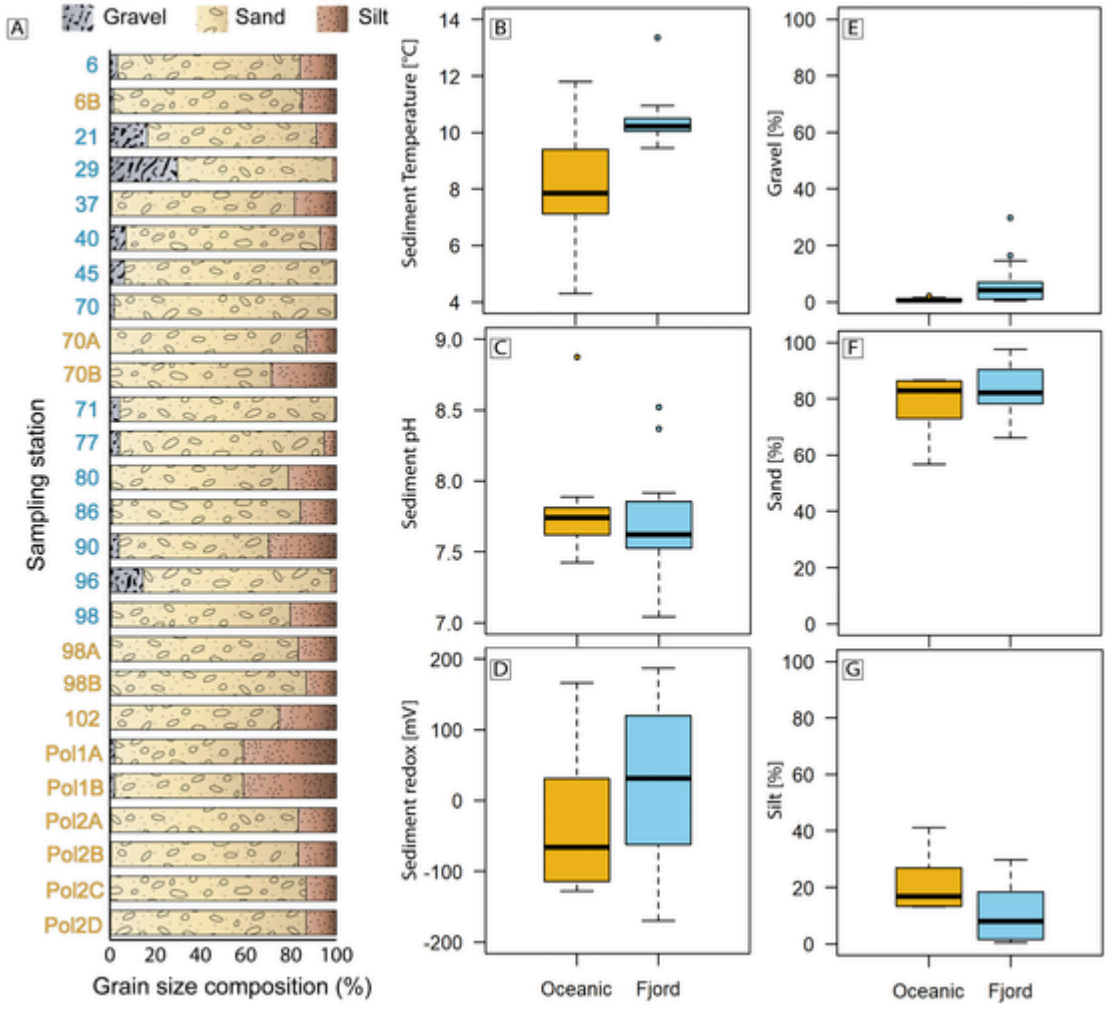

Fig. 3. A) Spatial variability of grain size composition (%) recorded at each sampling station. The numbered stations are the same as those shown in fig. 1. Boxplots of physicochemical characteristics in the fjord and oceanic environments. B) Sediment temperature (°C); C) pH: D) Redox potential (mV); E) Gravel; F) Sand and G) Silt grain size composition (%). The boxplots show a range (whiskers), median (bold line) and interquartile range (box height).

Finally, the sediments in the study area were mostly composed of fine sand (Fig. 3A). Specifically, the sediments from the oceanic and fjord environments showed gravel median values of 0.41% (IQR = 0.47), and 4.11% (IQR = 5.50), respectively (Fig. 3E). Sand records revealed median values of 82.66% (IQR = 12.44) for the oceanic and 82.01% (IQR = 10.84) for the fjord environment (Fig. 3F). Silt presents the most notable difference in grain size composition in which oceanic displayed median values of 16.81% (IQR = 12.76) and the fjord environment 7.91% (IQR = 16.10) (Fig. 3G).

3.2. Chemical conditions of the water column

Although with certain spatial heterogeneity, nitrate (Fig. 4A, B), phosphate (Fig. 4C, D) and silicates (Fig. 4E, F) —the nutrients that have a more conservative behavior— presented different distribution patterns, while the silicate showed a conservative behavior in an estuarine regime, the nitrate and phosphate show a certain accumulation in the interior sea or inland sea. It is known that oceanic waters have intermediate levels of nitrate and phosphate typical of Subantarctic Water (SAAW) and that river waters (freshwater discharge) did not have detectable levels of either nutrient (Sievers and Silva, 2008; Silva and Calvete, 2002).

Thus, the highest and lowest nitrate values were recorded in stations 71 (11.985 μM l^{-1}) and 86 (1.463 μM l^{-1}), respectively (Fig. 4A). The nitrate oceanic median was 7.29 (IQR = 2.62), lower than the fjord environment median of 9.28 (IQR = 1.39) (Fig. 4B). Higher phosphates were principally observed in the inland sea of Chiloé and the fjords of the Aysén region (Fig. 4C). The highest and lowest phosphate values were recorded in the sampling stations 96 (1.24 μM l^{-1}) and 86 (0.076 μM l^{-1}), respectively (Fig. 4C). The phosphate oceanic median was 0.86 (IQR = 0.23), lower than the fjord environment median of 1.01 (IQR = 0.20) (Fig. 4D). The silicate showed the highest values (52.718 μM l^{-1}) in the Aysén fjord station 80, and the lowest in the oceanic station 70B (2.092 μM l^{-1}) (Fig. 4E). Silicate showed an inverse behavior with salinity, as is well known, the highest input came from continental runoff (Torres et al., 2014). The silicate oceanic median was 4.22 (IQR = 1.84), lower than the fjord environment median of 7.79 (IQR = 2.72) (Fig. 4F).

Regarding nitrite and ammonium, nutrients that rarely accumulate in the ocean and are found in submicromolar concentration ranges, both showed heterogeneous distributions and at levels below 0.35 and 3.15 uM l^{-1}, respectively. Nitrites showed higher values mostly in the oceanic environment specifically in stations 102 (0.345 μM l^{-1}) and 70A (0.328 μM l^{-1}) (Fig. 4G). Notwithstanding, similar values were observed in station 71 (0.345 μM l^{-1}) with high oceanic influence (Fig. 4G). The nitrites oceanic median was 0.24 (IQR = 0.08), higher than the fjord environment median of 0.22 (IQR = 0.11) (Fig. 4H).

The high levels of ammonium were surprising as they were not expected for either continental and oceanic waters in the northern Patagonia region; they seem to have arisen from regenerative processes (decomposition of organic matter). Indeed, the highest and lowest ammonium values were recorded in the Puyuhuapi fjord stations 90 (3.15 μM l^{-1}) and 86 (0.44 μM l^{-1}), respectively (Fig. 4I). The ammonium oceanic median was 0.78 (IQR = 0.33), higher than the fjord median of 0.61 (IQR = 0.17) (Fig. 4J).

3.3. Diversity and abundance of dinoflagellate benthic cysts and meiofauna

The analysis of the sediment revealed a high genera richness of dinoflagellate benthic cysts, with *Protoperidinium* as the most important genus (Table 1, Fig. 5). The other genera recorded were: *Alexandrium, Protoceratium, Gonyaulax, Lingulodinium, Pentapharsodinium, Scrippsiella, Archaeperidinium, Polykrikos, Preperidinium, Diplopsalopsis* and *Niea* (Table 1, Fig. 5). Forty-four different dinoflagellates cyst morphotypes were identified, 30 of which were identified to species level (Table 1, Fig. 5). Two species (*Polykrikos kofoidii* and *Archaeperidinium constrictum*) were not observed in the fjord system and seven species (all unidentified) were not found in the oceanic environment (Table 1).

Dinoflagellate benthic cysts were found at all sampling stations, and their total abundances ranged from 4 to 3633 cysts cm^{-3} (1686 ± 2524; n = 26) (Table 1). The highest cysts abundances were found in the Puyuhuapi Fjord, Aysén region (Fig. 6A). HAB species were observed in both fjords and oceanic environments. *Alexandrium catenella* (saxitoxin producer) cysts were found at 12 sampling stations with abundances from 4 to 68 cysts cm^{-3} (14.2 ± 22.1; n = 26) (Fig. 6B). The abundances of the following yessotoxins producer species identified were: *Protoceratium reticulatum* with 5–312 cysts cm^{-3} (33.5 ± 75.6; n = 26); Fig. 5C), *Gonyaulax spinifera* with 11–253 cysts cm^{-3} (39.1 ± 68.1; n = 26), and *Lingulodinium polyedrum* with 12–180 cysts cm^{-3} (13.0 ± 42.8 std.; n = 26). Interestingly, empty cysts of *P. reticulatum* were found at 25 of the 26 sampling stations, with a total maximum abundance of 9361 empty cysts cm^{-3} (676.0 ± 1879.0; n = 26) at Puyuhuapi Fjord (est.86) (Fig. 6D).

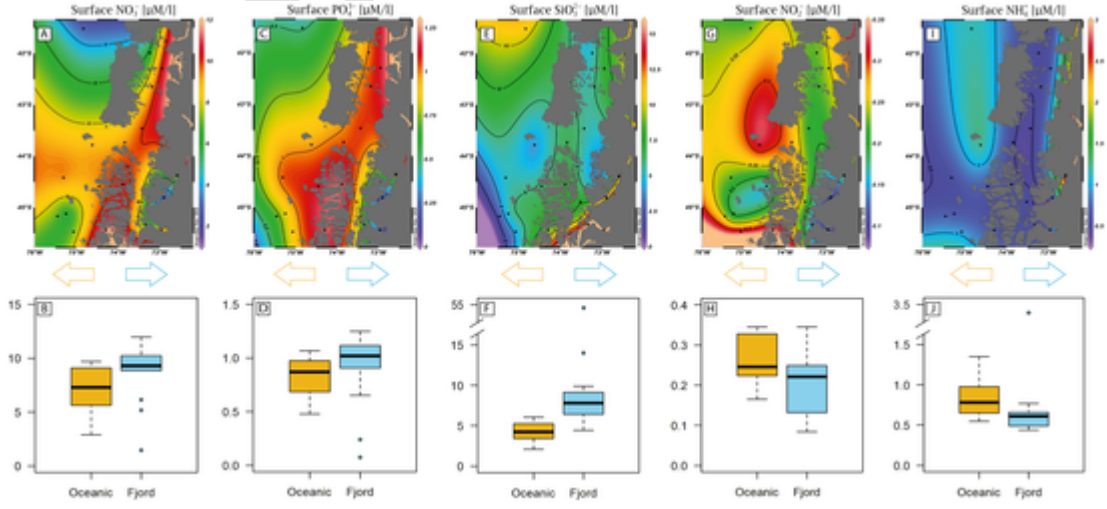

Fig. 4. Spatial variability of surface inorganic nutrients in the study area. A-B) nitrates (NO_3^-); C–D) phosphates (PO_4^{3-}); E–F) silicates (SiO_3^{2-}); G–H) nitrites (NO_2^-); I–J) ammonium (NH_4^+). The boxplots for oceanic and fjord environments show a range (whiskers), median (bold line) and interquartile range (box height).

Table 1
Nutritional strategy (a: autotroph; h: heterotroph) and mean abundance (cysts cm^{-3}) of 44 types of dinoflagellate resting cysts recorded during the 2018 CIMAR 24 oceanographic campaign. The abundance of empty dinoflagellate resting cysts is shown in parenthesis.

Sampling station	NS	Code	Fjord system														Oceanic system							
			6	21	29	37	40	45	70	71	77	80	86	90	96	98	6 B	102	70 A	70 B	98 A	98 B	Pol 2A	Pol 2B
Depth [m]			294	163	97	250	180	83	78	159	212	197	286	35	246	168	1074	243	131	315	49	225	225	1070
Gonyaucales																								
Alexandrium catenella (Wedon & Kofoid) Balech	a	Acat	0	0	0	33	66	27	0	4	15	0	66	0	5	68	0	32	22	0	0	14	0	0
Protoceratium reticulatum (Claparece & Lachmann) Bütschli	a	Pret	10 (150)	0 (5)	0 (5)	55 (1254)	61 (3020)	0 (23)	0 (6)	0 (4)	25 (530)	0 (21)	242 (9362)	312 (540)	0 (77)	27 (806)	0 (36)	8 (160)	0 (143)	5 (67)	0	0 (108)	60 (390)	0 (180)
Gonyaulax spp. (*Spiniferites_pachydermus*)	a	Gspa	0	0	0	0	0	0	0	0	0	0	88	0	0	0	5	0	0	10	0	0	20	0
Gonyaulax spp. (*Spiniferites_ramosus*)	a	Gsra	170	0	0	0	44	0	0	0	0	0	22	0	0	0	5	48	77	48	0	50	200	36
Gonyaulax spp. (*Impagidinium patulum*)	a	Gipa	0	0	0	0	0	0	0	0	0	0	0	0	0	0	5	0	0	0	0	0	0	9
Gonyaulax spinifera (*Nematosphaeropsis_labyrinthus*) (Claparece & Lachmann)	a	Gspi	0	4	0	11	0	0	0	0	0	0	0	0	0	0	27	24	11	124	0	27	170	108
cf. *Lingulodinium polyedrum* Gymndiniales	a	Lpol	0	0	0	0	0	0	0	0	0	0	0	12	0	0	0	0	0	14	0	0	180	0
Polykrikos schwartzii Bütschli	h	Psch	90	0	9	121	259	5	3	4	55	10	352	0	3	113	81	168	55	133	0	81	290	225
Polykrikos kofoidii	h	Pkof	0	0	0	0	0	0	0	0	0	0	0	0	0	0	0	0	0	0	0	0	30	0
Polykrikos sp.1	h	Psp1	0	0	0	22	0	0	0	0	0	10	0	0	0	9	0	0	11	14	0	9	50	9
Peridiniales																								
Pentapharsodinium dalei indelicato *et* Loeblich III	h	Pdal	20	0	7	44	6	0	0	0	0	0	330	0	0	14	9	8	66	19	0	9	20	0
Scrippsiella trochoidea (Stein) Loeblich III	a	Stro	0	0	0	0	0	0	0	0	0	0	0	0	0	5	0	0	0	0	0	0	0	5
*Scrippsiella patagonica*Akselman *et* Keupp	a	Spat	0	0	0	22	0	0	0	0	0	0	0	0	0	0	0	4	0	0	0	0	10	0
Archaeperidinium minutum (Kofoid) Jørgensen	h	Amin	930	4	68	407	160	27	0	0	70	10	506	144	11	162	81	108	22	33	0	32	180	144
Archaeperidinium constrictum (Abé)	h	Acon	0	0	0	0	0	0	0	0	0	0	0	0	0	0	0	12	0	0	0	0	0	9
Protoperidinium americanum (Gran & Baraaud) Balech	h	Pame	210	0	7	341	132	0	0	1	10	0	176	12	0	41	135	164	121	119	2	77	55	279
Protoperidinium avellana (Meunier) Balech	h	Pave	160	2	9	198	127	15	0	0	55	44	341	0	5	63	54	108	44	76	2	63	190	72
Protoperidinium claudicans (Paulsen) Balech	h	Pcla	30	0	0	11	22	0	0	0	10	0	0	12	0	5	5	12	0	0	0	9	10	5
Protoperidinium conicoides (Gran) Balech	h	Pcon	110	0	0	55	33	0	0	0	5	10	110	0	5	9	50	36	11	14	0	14	60	72
Protoperidinium conicum (Gran) Balech	h	Pcni	10	2	2	110	253	9	0	0	105	0	154	24	5	45	23	44	88	19	0	36	50	54
Protoperidinium denticulatum (Gran & Baraaud) Balech	h	Pden	30	0	2	77	50	0	0	0	10	10	66	0	0	14	14	92	11	10	0	41	100	90
Protoperidinium excentricum (Paulsen) Balech	h	Pexc	150	0	12	55	110	0	0	4	50	131	198	24	5	54	27	52	11	24	0	23	40	32

Sampling station	NS	Code	Fjord system													Oceanic system									
			6	21	29	37	40	45	70	71	77	80	86	90	96	98	6 B	102	70 A	70 B	98 A	98 B	Pol 2A	Pol 2B	Pol 2C	Pc 2I
Depth [m]			294	163	97	250	180	83	78	159	212	197	286	35	246	168	1074	243	131	315	49	225	225	1070	1619	33
Protoperidinium leonis (Pavillard) Balech	h	Pleo	20	2	2	33	17	0	0	0	0	32	22	0	0	18	14	52	66	33	0	50	80	27	110	23
Protoperidinium cf. *nudum*	h	Pnud	20	0	0	0	50	0	0	0	10	0	0	0	3	45	0	16	0	0	0	0	40	18	33	0
Protoperidinium oblongum	h	Pobl	0	0	0	0	0	5	0	0	45	0	0	0	0	0	0	8	0	0	0	0	0	0	0	0
Protoperidinium pentagonum (Gran) Balech	h	Ppen	10	0	7	55	39	10	0	0	35	21	132	0	0	18	0	36	11	19	0	0	20	9	33	8
Protoperidinium subinerme (Paulsen) Loeblich III	h	Psub	40	0	2	66	39	0	0	0	5	0	22	0	3	32	23	40	22	29	0	9	80	54	44	53
Protoperidinium spp.	h	Pspp	100	2	5	33	11	9	3	0	15	21	88	48	0	27	14	24	22	5	0	18	0	36	11	0
Protoperidinium sp.5	h	Psp5	0	0	0	22	0	0	0	0	0	0	0	0	0	0	0	0	0	0	0	0	0	0	11	0
Protoperidinium sp.6	h	Psp6	0	0	0	0	0	5	0	0	0	0	0	12	3	0	0	0	0	0	0	0	0	0	0	0
Preperidinium meunieri	h	Pmeu	30	2	5	88	72	5	0	4	10	32	66	12	3	14	5	64	11	0	0	0	20	45	0	15
Diplopsalopsis ovata (Abé)	h	Dova	10	0	2	0	0	0	0	0	0	0	0	0	0	0	0	0	0	0	0	0	30	9	0	0
Niea acanthocysta (Kawami, Iwataki & Matsuoka)	h	Naca	0	0	0	22	17	5	0	0	15	0	22	12	0	14	23	0	0	19	0	18	0	27	0	0
Unidentified cysts																										
Unidintified 1		Un01	10	2	2	0	0	0	0	0	5	10	22	36	0	9	0	0	0	0	0	0	0	0	0	0
Unidintified 2		Un02	40	0	0	0	28	0	0	0	35	55	0	24	0	27	0	8	0	0	0	0	0	0	0	0
Unidintified 8		Un08	0	0	0	0	0	0	0	0	5	0	0	0	0	14	0	0	0	0	0	0	0	0	0	0
Unidintified 9		Un09	0	0	0	11	6	0	0	0	0	32	0	156	0	0	9	0	0	0	0	0	0	18	11	0
Unidintified 10		Un10	0	0	0	0	0	0	0	0	20	0	0	0	0	0	0	0	0	5	0	0	0	0	0	0
Unidintified 13		Un13	30	0	2	0	0	0	0	0	0	10	0	0	0	0	0	0	0	0	0	0	0	0	0	0
Unidintified14		Un14	20	0	0	0	11	0	0	4	0	44	0	204	0	0	0	0	0	0	0	0	0	0	0	0
Unidintified15		Un15	0	0	0	0	0	5	0	0	0	0	0	0	0	0	0	0	0	0	0	0	0	0	0	0
Unidintified 19		Un19	0	0	0	0	0	0	0	0	5	0	0	0	0	0	0	0	0	0	0	0	0	0	0	0
Unidintified 26		Un26	0	0	0	0	0	0	0	0	0	0	0	36	0	0	0	0	0	0	0	0	0	0	0	0
Unidintified 34		Un34	60	2	0	165	132	0	0	11	25	0	198	0	8	50	5	80	22	5	0	32	100	149	44	0

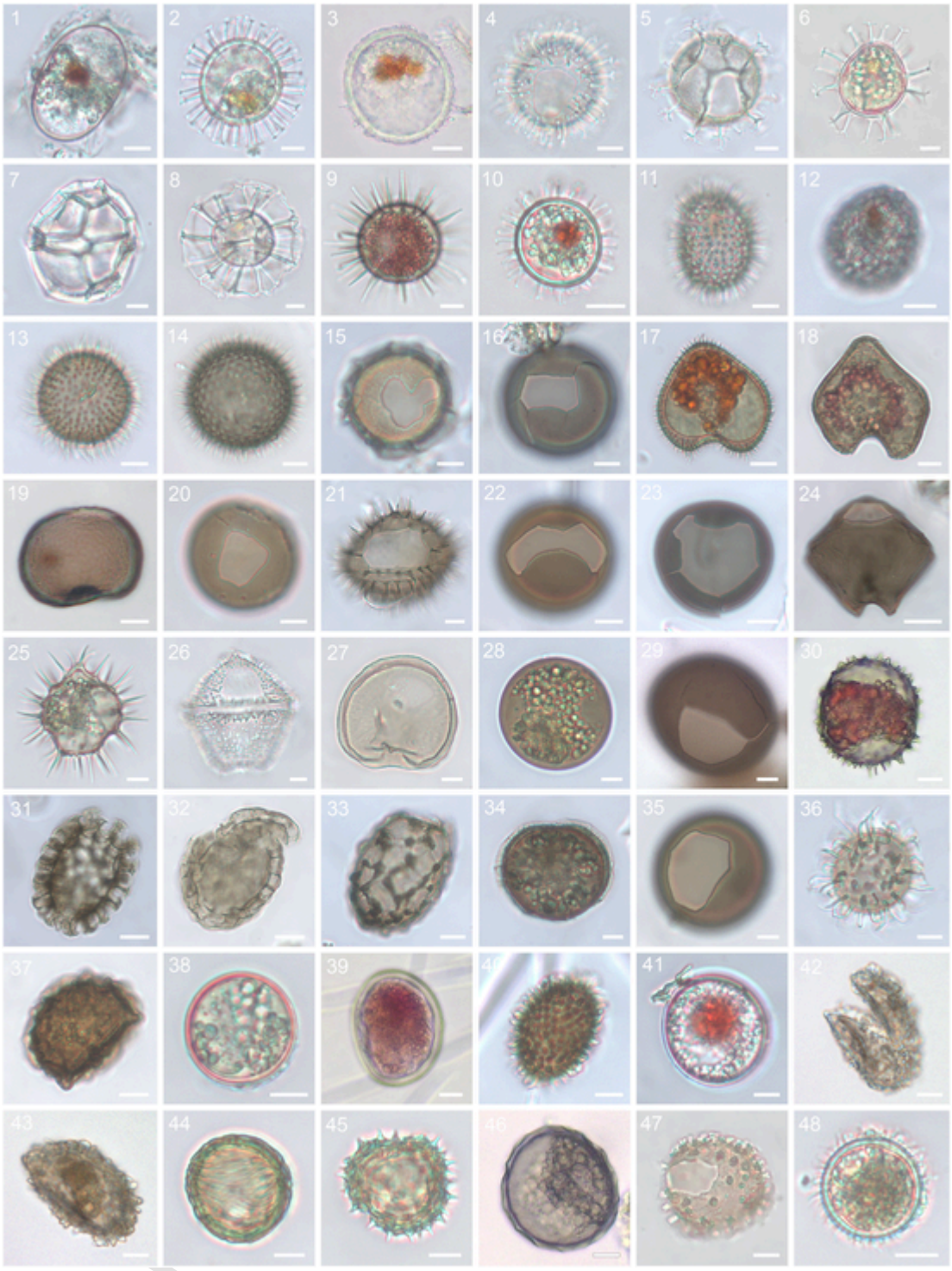

Fig. 5. Dinoflagellates cysts species richness in surface recent sediments of Los Lagos and Aysén regions. 1) *Alexandrium catenella*; 2) *Protoceratium reticulatum*; 3) *P. reticulatum* without processes; 4) *P. reticulatum* Empty cyst; 5) *Spiniferites* cf. *pachydermus*; 6) *Spiniferites* cf. *ramosus*; 7) *Impagidinium patulum*; 8) *Nematosphaeropsis labyrinthus*; 9) *Lingulodinium polyedrum*; 10) *Pentapharsodinium dalei*; 11) *Scrippsiella trochoidea*; 12) *Scrippsiella patagonica*; 13) *Archaeperidinium minutum*; 14) *Archaeperidinium constrictum*; 15) *Protoperidinium americanum*; 16) *Protoperidinium avellana*; 17) *Protoperidinium claudicans*; 18) *Protoperidinium oblongum*; 19–20) *Protoperidinium conicoide*; 21) *Protoperidinium conicum*; 22) *Protoperidinium denticulatum*; 23) *Protoperidinium excentricum*; 24) *Protoperidinium leonis*; 25) *Protoperidinium* cf. *nudum*; 26) *Protoperidinium pentagonum*; 27) *Protoperidinium subinerme*; 28) *Protoperidinium* spp.; 29) *Protoperidinium* sp. 5; 30) *Protoperidinium* sp. 6; 31) *Polykrikos schwartzii*; 32) *Polykrikos kofoidii*; 33) *Polykrikos* sp. 1; 34) *Preperidinium meunieri*; 35) *Diplopsalopsis ovata*; 36) *Niea acanthocysta*; 37) unidentified 1; 38) unidentified 2; 39) unidentified 8; 40) unidentified 9; 41) unidentified 10; 42–43) unidentified 13; 44) unidentified 14; 45) unidentified 15; 46) unidentified 19; 47) unidentified 26; 48) unidentified 34.

Total meiofauna abundance ranged between 49 and 3887 ind./10 cm^2 (1209.9 ± 1224.0; n = 21) (Fig. 7A). The most abundant group was the Nematoda with 53–3222 ind./10 cm^2 (997.6 ± 1026.9; n = 21) (Fig. 7D), followed by Foraminifera with 5–641 ind./10 cm^2

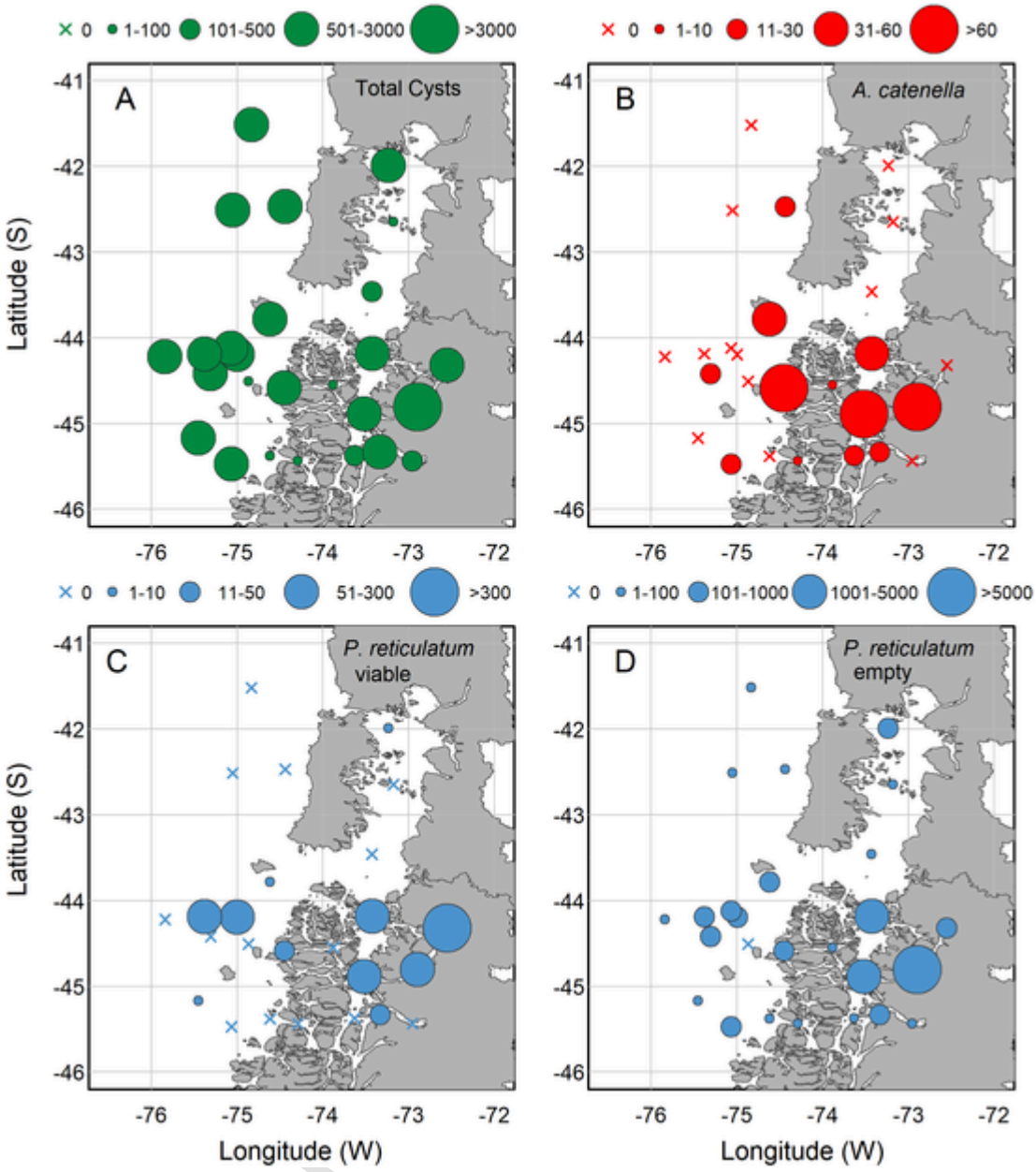

Fig. 6. Spatial variability in dinoflagellates cysts assemblages in the study area. A) Total dinoflagellates cysts abundance. B) *Alexandrium catenella* cysts abundance. C) *Protoceratium reticulatum* (viable) cysts abundance. D) *Protoceratium reticulatum* (empty) cysts abundance.

(142.0 ± 181.9; $n = 21$) (Fig. 7B), and Harpacticoida with 1–158 ind./10 cm^2 (31.8 ± 37.6; $n = 21$) (Fig. 7C).

The nMDS ecological community analysis display marked differences in the species composition dinoflagellate benthic cysts between the fjord and oceanic environments, with a clear separation between them even though a smooth overlap can be observed (Stress = 0.07; Fig. 8A). Moreover, ANOSIM analysis gave strong support ($p = 0.011$) to the hypothesis that dinoflagellate benthic cyst assemblages are different between fjords and oceanic environments (Fig. 8B). The highest contribution to the dissimilarity between environments (values ≥6%) was attributed to the contributions of the species: *P. americanum*, *A. minutum*, *P. schwartzii*, and *P. avellana* (Fig. 8C). This finding is also supported by the variation in cysts abundances observed for each species in Fjord and Oceanic environments (Fig. 8D, E). The PERMANOVA indicated that sediment temperature ($p = 0.0399$) and silt proportion ($p = 0.0366$) had a strong influence upon species composition of dinoflagellate benthic cysts communities within the study area (Table 2), followed by sand proportion ($p = 0.085$) and Foraminifera abundance ($p = 0.068$).

The GLM adjusted model for *A. catenella* showed that redox, sediment temperature, silt, sand, and Harpacticoida copepods explained significantly ($p < 0.05$) a large fraction of the spatial variability of their cysts abundance. No evidence of large effects of sediment pH and the remaining meiofaunal groups (Nematode and Foraminifera) were found (Table 3).

4. Discussion

Many dinoflagellate species form cyst stages in order to cope with both short and long term environmental variation, sinking to the seafloor where they can become inoculum for fueling subsequent

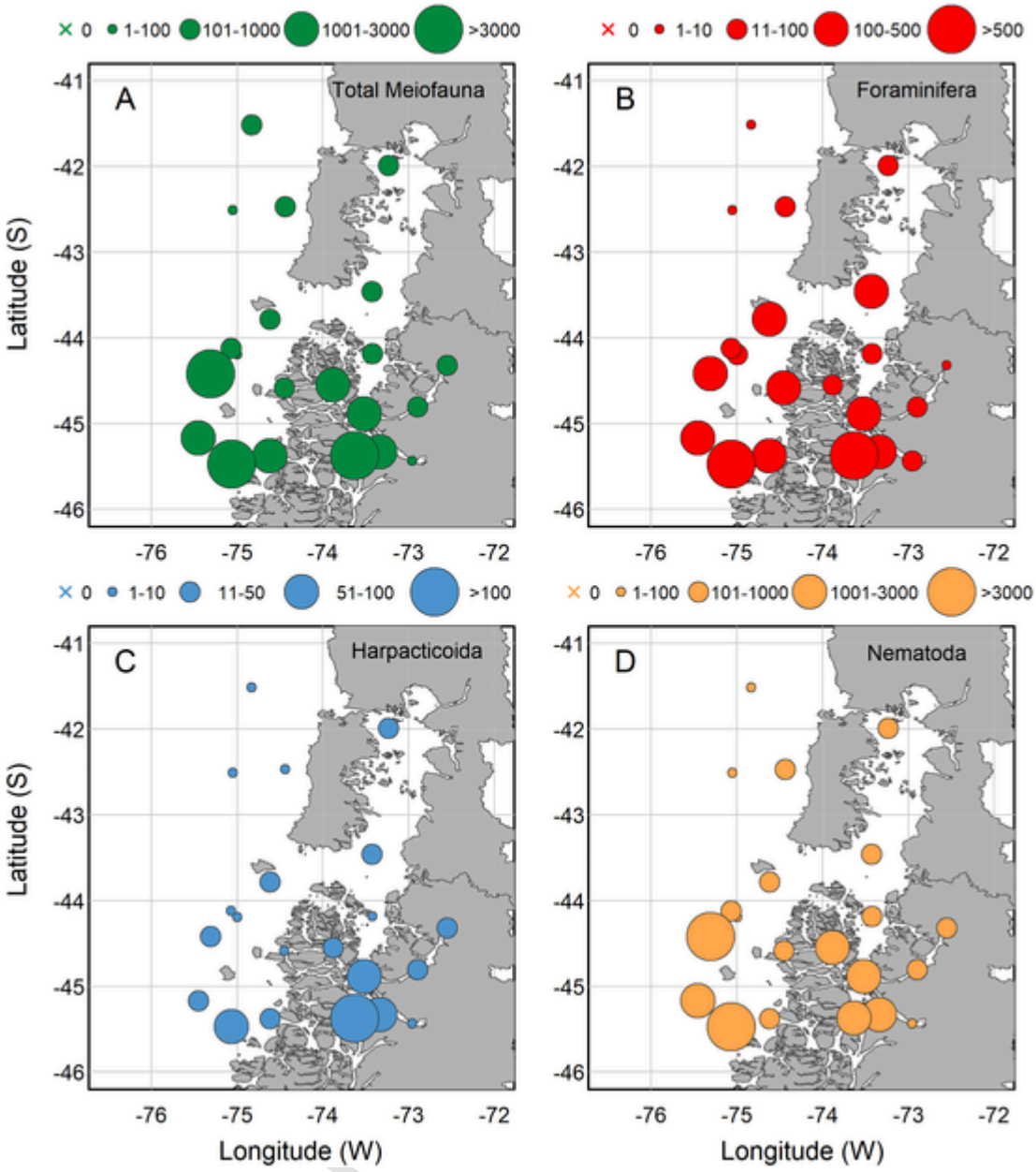

Fig. 7. Spatial variability in meiofauna assemblages in the study area. A) Total meiofauna abundance; B) Foraminifera abundance; C) Harpacticoida abundance and D) Nematoda abundance.

blooms (Anderson et al., 1983; Matsuoka, 1999; Mudie et al., 2002; Nehring, 1993; Pati et al., 1999). These species may spend the majority of their lives in sediments as cysts, waiting for optimal germination conditions (Brosnahan et al., 2020; Fryxell, 1983; Kremp et al., 2016). It is therefore extremely important to determine the hotspots of cyst accumulation as they are likely pointing to where new blooms could start (Brosnahan et al., 2020; McGillicuddy et al., 2011).

Twenty years ago, a theoretical framework for ecological interactions between cysts (seed banks), and the physicochemical characteristics of the sediment, the bioturbation by larger fauna, and the impact of potential cyst predators was proposed (Persson, 2000), but many of these interactions remain to be explored. Here, using a biogeographic mesoscale approach in an area where PSP outbreaks are recurrent (NW Chilean Patagonia), we present patterns and specific drivers of resting cyst abundances associated with both ecological interactions and physicochemical characteristics in southern Chile. We also report the first observations of the harmful resting cysts of *A. catenella*, *P. reticulatum*, *G. spinifera* and L. *polyedrum* on the adjacent oceanic shelf in north-western Chilean Patagonia.

4.1. Drivers of resting cyst assemblages

The samples collected in the oceanographic campaign revealed the existence of 12 different genera as part of two different cyst assemblages located in the fjord and oceanic environments, associated with two specific drivers: sediment temperature and the presence of high proportions of silt (Fig. 8B; Table 2). Our results reveal that higher temperatures and lower silt content characterize fjords, whereas lower temperatures and higher silt content characterize the oceanic environment. Between the two environments, it was possible to identify a median difference in sediment temperature of ~2.8 °C, and a difference of

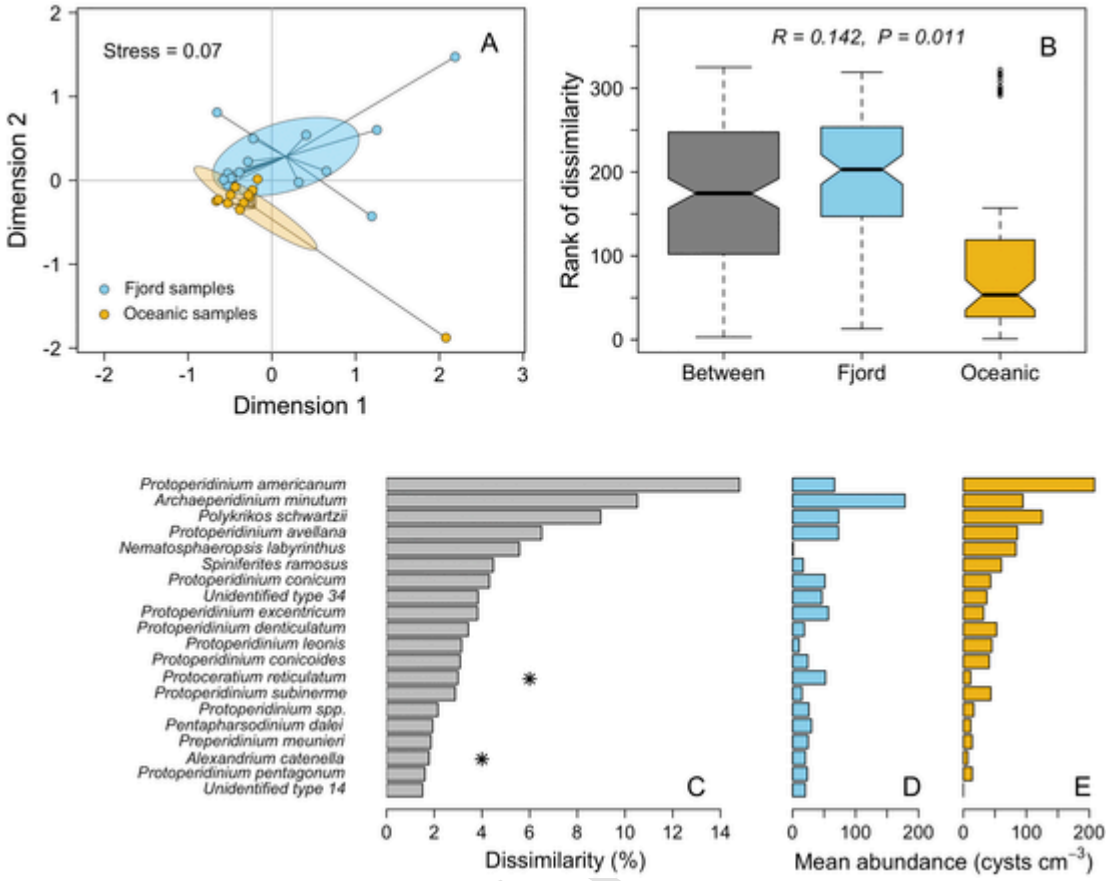

Fig. 8. A) Two-dimensional representation of the nMDS analysis; B) Box-plot diagram of the ANOSIM results; C) Dinoflagellate resting cysts with the greatest contributions to the average dissimilarity of the assemblages at the fjord and oceanic samples based on a SIMPER analysis; D-E) Mean abundance (cysts cm^{-3}) per dinoflagellate species as determined fjord (D) and oceanic (E). The asterisk (*) indicates harmful species.

Table 2
PERMANOVA based on Bray-Curtis dissimilarities of physical-chemical properties of sediment and meiofauna groups over the resting cysts community (48 species) using 10.000 permutations for the hypothesis test. Significant effects ($p < 0.05$) are shown by an asterisk.

Predictive variables	DF	Sum of squares	R^2	Pseudo-F	*Pr > F*
Redox	1	0.332	0.0459	1.532	0.1198
Sediment temperature	1	0.438	0.0606	2.021	0.0399*
Sediment pH	1	0.271	0.0374	1.249	0.2269
Silt	1	0.461	0.0637	2.124	0.0366*
Sand	1	0.381	0.0527	1.756	0.0855
Foraminifera	1	0.391	0.0541	1.803	0.0680
Harpacticoida	1	0.255	0.0352	1.175	0.2984
Nematoda	1	0.116	0.0161	0.536	0.9183
Residuals	18	3.691	0.5101		
Total	25	7.235	1.0000		

Table 3
Statistical significance of explanatory variables determined using an X^2 test of marginal (type II) ANOVA for the variability of toxic dinoflagellate *Alexandrium catenella* in the sediment, using a generalized Lineal Model (GLM) with logit link function for the residual negative binomial distribution. Significant effects ($p < 0.05$) are shown by an asterisk.

Alexandrium catenella			
Predictive variables	Chi square X^2	DF	*Pr* > ($\|X^2\|$)
Redox	3.855	1	0.0495*
Sediment temperature	5.143	1	0.0233*
Sediment pH	0.016	1	0.8987
Silt	4.094	1	0.0430*
Sand	4.620	1	0.0315*
Foraminifera	1.442	1	0.2297
Harpacticoida	4.104	1	0.0427*
Nematoda	0.633	1	0.4261

8.9% in silt proportion (Fig. 3B,G), which show a significant association with the observed differences in cyst assemblages.

Following the main hypothesis about the preferable origin of blooms in the area (Díaz et al., 2014), the presence of cysts in the sediments of the oceanic areas is probably a result of long distance transport from the interior of fjords and channels. Thus, this potential "seed bank cysts" as suggested Mardones et al. (2016) could be resuspended by oceanographic processes and be transported back into the fjord system. As consequence, within the fjords and channels, the cysts are likely transported over much shorter distances (Dale and Dale, 1992). This spatial distribution pattern of resting cyst assemblages has been observed in other areas of the world such as in Manila bay and Bizerte lagoon with an identified tendency to decrease in abundance from protected (e.g. fjords) to exposed areas (e.g. oceanic) (Azanza et al., 2004; Fertouna-Bellakhal et al., 2014).

Typically, the spatial distribution of dinoflagellate resting cysts in the sediments is patchy and heterogeneous. Several studies have revealed that temperature can be important in explaining the distributions of resting cysts assemblages (e.g. Fertouna-Bellakhal et al.,

2014; Price et al., 2016). Species-specific tolerances and/or adaptations to cooler (oceanic) or warmer (fjord) environments could underlie the observed differences in assemblages (Kremp et al., 2016). Consequently, knowledge of the sediment temperature and the temperature tolerances of the different species present in a region could indicate the combination of species that will be found in the sediment at a specific location (Marret and Zonneveld, 2003). For example the cysts of the species *Pyrodinium* spp. —a saxitoxin producer— have been found to dominate in areas where the temperatures are unfavorable for germination (Azanza et al., 2004; Ellegaard and Ribeiro, 2018). Precaution, however, should, be taken when applying this assumption, as sediment temperature is not constant and the observed cyst assemblages are the result of the accumulation of cysts from different cohorts over time that exhibits distinct genetic and physiological characteristics (Ribeiro et al., 2013).

According to our results, the contribution of the harmful species *P. reticulatum* and *A. catenella* to the dissimilarity between environments was second only (with higher values in fjords than in the oceanic environment that will be discussed below), to that of the harmless species *Protoperidinium americanum* and *Archaeperidinium minutum* (Fig. 8C–E). The pattern detected indicates that the abundance of *A. minutum* was higher in fjords than in the oceanic environment. Conversely, the abundance of *P. americanum* was higher in the oceanic environment than in the fjords. This coincides with the known distribution of *P. americanum* in coastal sub-polar to tropical regions where eutrophic conditions such as those generated by upwelling dominate, and also its infrequency in areas of low salinity, such as those found in the austral fjords (Zonneveld et al., 2013). In the Aysén fjords, the highest abundance recently observed was a mean of 1 cm^{-3} (Díaz et al., 2018). Although *Archaeperidinium minutum* has a worldwide distribution (Guiry, 2020), optimal growing conditions have been related to enhanced rainfall and freshwater inputs. Accordingly, our results indicate that it is most abundant in fjord environment, confirmed by the recent observation of its presence in low abundances in the Aysén region (Díaz et al., 2018).

Cyst abundance has been related to sediment type and grain size. In this sense, higher content of finer-grain-size fractions (clay and/or silt) in the sediment appears to be an important indicator of the likelihood that the sediment will contain high abundances of cysts (Dale, 1976; Nehring, 1993; Olli and Trunov, 2010). Hydrodynamic conditions that result in the accumulation of fine sediments will also govern the settlement of cysts, which behave as passive sediment particles with similar characteristics. Following this trend, we found a positive correlation between the higher silt content and the mean abundance of several species as observed in the oceanic environment (Fig. 8D–E), which contained ~8.9% higher silt content relative to fjords (Fig. 3G). In a previous comparison of the cyst distributions from a variety of environments (e.g., fjords, estuaries, shallow coastal embayments), an increase of cyst abundances and cyst species richness was associated with decreasing mean sediment grain size (Nehring, 1993). This supports our observations of the differences in cyst assemblages between the oceanic and fjord environments given that the dominant fraction of the sediment in both environments was fine sand (median ~ 82%), finding a higher percentage of silt in the oceanic environment (Fig. 3).

A last and unconsidered effect in this study is the effect of anthropogenic impact on resting cyst assemblages. In general, fjords and estuaries experience greater variation in temperature, salinity, and pollution than in the oceanic environment. Previous studies have revealed that cyst assemblages can differ in polluted environments relative to more pristine environments, with a decline in autotroph species in metal-polluted areas (Azanza et al., 2004; Sætre et al., 1997). Considering the high aquaculture pressure in NW Patagonia with >95% mussel production (30×10^4 t y^{-1}) and salmon industry with high contribution to the $>80 \times 10^4$ t y^{-1} (SalmonChile, 2018; Sernapesca, 2017), our results could be ideal to prove aquaculture externality to a sedimentary environment and enhance the understanding of potential HABs development in this productive area.

4.2. Nutrients and resting cyst deposits

Nutrients may affect the size of resting cysts deposits on two different levels. Firstly, laboratory experiments indicate that sexuality, and consequently resting cyst production, is enhanced when the blooming population depletes the nutrients that are necessary to sustain its growth, providing that enough reserves of nitrates and phosphates have been previously stored in the cells to allow for the viability of zygotes and resting cysts (e.g. see review in Figueroa et al., 2018). Following this premise, a certain similarity can be observed between the abundance patterns of nitrates and phosphates (Fig. 4A and E) and that of total resting cysts (Fig. 6A). This relationship must be treated with care, as resting cysts deposits represent a serial cohort of cysts, most probably of different ages and from different bloom events, which together with the dynamics of currents in a given area, may have more of an effect on the final location and abundance of resting cysts than this potential nutritional factor. Secondly, nutrients may also be relevant once resting cysts are formed. During post-encystment, nutrient levels not only directly determine the viability of the germinated cells, but could also affect the development and germination time of resting cysts. Besides being stages of low metabolic activity, resting cysts could take up nutrients such as phosphorous in order to complete their dormancy requirements, speed up germination time and increase their germination success (Binder and Anderson, 1987; Rengefors et al., 1996). However, this effect has not always been demonstrated, as the dilution of the culture medium, or the lack of N and P nutrients, do not appear to decrease germination success in the *Alexandrium tamarense* species complex (Figueroa et al., 2005; Genovesi et al., 2009). Moreover, given that other factors directly prevent resting cyst germination (such as dormancy requirements, anoxia and sediment resuspension), and presuming that nutrient levels are constantly changing (both in time and depth), evaluating the relevance of nutrients in the germination of a complex pool of resting cysts is difficult.

4.3. Drivers of Alexandrium catenella resting cysts and the two hypotheses

In marine sediments, the cysts experience a variable environment and germination takes place when the temperature, oxygen concentrations, nutrients and light levels are optimal. These conditions typically occur at the sediment surface or after resuspension of cysts from deeper sediment layers. When the conditions are suboptimal, with low temperatures, oxygen concentrations, and light levels, the cysts remain in a state of quiescence, even if the species-specific dormancy period was completed. Cysts that settle to the sediment surface are frequently rapidly buried via bioturbation of benthic invertebrates. Meiofauna plays an important role in this process due to their high abundance. Bioturbation will move the cysts randomly up and down in the sediment, and as germination can only take place at the sediment surface, cysts can remain buried in the sediment in a quiescent state for prolonged periods, in some cases even hundred years (Agrawal, 2009; Genovesi-Giunti et al., 2006; Montresor and Marino, 1996; Ribeiro et al., 2011). Our data highlight the relevance of the interactions between bioturbation and the environmental variability of the sediments, to directly influence the population dynamics of *A. catenella* resting cysts. In this regard, the main drivers influencing population dynamics in NW Patagonia are sediment redox potential, sediment temperature, granulometry, and Harpacticoida copepod abundance (Table 3).

The presence of *A. catenella* resting cysts in the sediments on the external continental shelf of the Lagos and Aysén regions could be a re-

sult of the intense summer bloom in 2016 (Armijo et al., 2020; Buschmann et al., 2016; Hernández et al., 2016). Their heterogeneous spatial distribution in the fjord and oceanic environments (Fig. 6B–D) is consistent with a patchy accumulation pattern previously described and that has been observed in the Los Lagos and Aysén regions in previous oceanographic expeditions (i.e., CIMAR cruises 1996–2010) and during/after the intense bloom in 2009 (Díaz et al., 2014; Mardones et al., 2016).

The spatial distribution of *A. catenella* described in this study correlates with specific areas of oxic and anoxic conditions in the sediments, with higher abundances of cysts being found in anoxic areas compared to oxygenated areas (Fig. 2I and 6B). Considering that oxygen is a requirement for the germination of resting cysts (Anderson et al., 1987; Ellegaard and Ribeiro, 2018; Kremp and Anderson, 2000), cysts settling on oxygenated sediments could germinate right after completing their minimum period of dormancy, not needing bioturbation, resuspension or any other oxygenating mechanism. In other areas in the world such as Puget Sound on the Pacific coast of the USA, *A. catenella* exhibited at least 150 days of dormancy (Horner et al., 2011). A field survey of resting cysts after the intense *A. catenella* bloom in the summer of 2009 in Chile, showed that the abundances of resting cysts in the sediment decreased due to germination or physical-biological interactions in the subsequent 90 days. In a laboratory study of Chilean strains of *A. catenella*, the lowest resting cyst dormancy period was 69 days at 10 °C (Mardones et al., 2016). As the minimum dormancy period is species-specific and endogenously regulated (Rengefors and Anderson, 2002), this difference between laboratory and field conditions could evidence an oxygen limitation in the sediments of some areas, assuming that no genetic differences between distant geographical strains are influencing the period of dormancy.

Resting cysts present in anoxic sediments should contain a mix of different cohorts (Ribeiro et al., 2013) that are unable to germinate due to the low oxygen concentrations and low constant temperatures (Ellegaard and Ribeiro, 2018; Kremp and Anderson, 2000). The result is the accumulation of cysts in anoxic sediments, which act as sinks, where cysts regulated by endogenous clocks undergo dormancy-quiescence cycles. Anoxia does not seem to have a negative effect on cyst germination success (Kremp and Anderson, 2000), with cysts preserving their viability even when buried as deep as 13 cm down in the sediment (Genovesi-Giunti et al., 2006). Additionally, some species such as *Alexandrium minutum*, could even need a short period of anoxia to allow resting cyst maturation (Figueroa et al., 2007). The sink populations of quiescent cysts can have a significant effect on bloom dynamics, when, through bioturbation or resuspension, large numbers of cysts are exposed to optimal germination conditions, which can trigger the formation of a harmful algal bloom (Kremp and Anderson, 2000).

Silt and sand texture as the driver of *A. catenella* resting cysts abundances in the study area are not clear at all. Indeed, the higher abundances of *A. catenella* resting cysts were positively correlated with silt but negatively correlated with sand in Puget Sound (Horner et al., 2011). Conversely, in the Aysén region, the *A. catenella* resting cysts abundances were associated with coarse sediment type as sand, gravel, or little stones (Díaz et al., 2018). Moreover, in a macroscale study of 10 years of *A. catenella* resting cysts surveys using an ecoregional approach from Magallanes (southernmost region) to the inland sea of Chiloé (northernmost region) with different oceanographic conditions, the highest cysts abundances were significantly associated with gravel, sand or mud according to the ecoregion analyzed (Rodríguez-Villegas et al. unpublished results). In this sense, sediment type as a specific *A. catenella* driver may be different from one place to another and for this reason seems to be bad predictor of *A. catenella* resting cysts abundances.

The low number of *A. catenella* resting cysts found in the oceanic area (max. 32 cysts cm^{-3}) could support the hypothesis proposing that the movements of deep water masses across the oceanic shelf could lead to the mass resuspension of resting cysts and thus the formation of blooms (Mardones et al., 2016). Hydrological connectivity plays an important role in marine environments (Godhe et al., 2016) and patches of sediment with low abundances of *A. catenella* resting cysts, such as those found in the oceanic environment in this study, can be resuspended and transported from offshore to inshore by physical processes such as upwelling or storms surges (Nehring, 1993). This favors the formation of "bottom cell clusters" as results of cysts geminating (Genovesi et al., 2009) with plastic growth performances (Paredes-Mella et al., 2020) as a result of exposure to oxygenated and warmer waters (Kremp and Anderson, 2000).

Concerning the second hypothesis (predation and/or bioturbation of meiofauna drive cyst distributions), thick or multi-layered cyst walls and their cover of mucilage increase their long term viability by reducing their vulnerability to predators and microbial degradation (Ellegaard and Ribeiro, 2018). According to our results, two observations suggest the possibility of interactions between meiofaunal organisms and the resting cysts of dinoflagellates. Firstly, there is a correlation between cyst abundances and harpacticoid abundances, with cyst abundances increasing with decreasing harpacticoid abundances (Fig. 6B and 7C). Secondly, there is a correlation between cyst abundance and sediment redox potential with cyst abundances increasing as sediment redox potential decreases. This might be evidence that the cysts are food items for the harpacticoid copepods, with anoxic sediments providing a spatial refuge from the harpacticoids because harpacticoid copepods are sensitive to low oxygen concentrations (Grego et al., 2014). Recent ingestion experiments using stable isotopes demonstrated that harpacticoid copepods do not differentiate between the cells of harmful (*Ostreopsis* cf. *ovata*) and harmless (*Amphidinium* cf. *carterae*) benthic dinoflagellates in the presence of other potential food items (diatoms) (Boisnoir et al., 2020). Harpacticoid copepods are a predominantly herbivorous group (De Troch et al., 2012) thus it is a reasonable assumption that they can feed on *A. catenella* resting cysts (Pati et al., 1999; Persson, 2000), and thus influence population dynamics of this dinoflagellate.

These findings provide some evidence to support the hypothesis that there are interactions between meiofaunal organisms and the resting cysts of dinoflagellates (particularly with *A. catenella*). These interactions may influence the types of sediment where cysts can accumulate and thus the areas that may initiate HABs when the overlying oceanographic conditions are favorable.

5. Conclusions

In this study, we used the combination of hydrographic (temperature, salinity, and dissolved oxygen), sediment physical-chemical properties (temperature, pH, and Redox potential), and meiofauna abundance and diversity –as sediment bioturbation organisms and potential cysts predators– for a holistic investigation of dinoflagellates cyst distribution, principally for *Alexandrium catenella*, in a high PSP outbreaks recurrence area in southern Chile. Harmful species like *A. catenella* showed a strong association with sediment oxygen concentrations. The highest cysts densities were found in anoxic areas and the lowest densities in oxygenated areas. Future research is needed to further refine the different ecological interactions and population dynamics of cysts in oxic and anoxic environments. This study, carried out in a region prone to recurrent PSP outbreaks, revealed that biological interactions between the meiofauna and dinoflagellate cysts likely play an important role in shaping cyst assemblages, and should be considered in future research.

CRediT authorship contribution statement

Camilo Rodríguez-Villegas: Conceptualization, Methodology, Software, Validation, Formal analysis, Investigation, Resources, Writing – original draft, Writing – review & editing, Visualization. **Matthew R. Lee:** Methodology, Software, Validation, Formal analysis, Investigation, Writing – original draft, Writing – review & editing. **Pablo Salgado:** Conceptualization, Methodology, Formal analysis, Writing – review & editing, Visualization. **Rosa I. Figueroa:** Conceptualization, Methodology, Software, Validation, Formal analysis, Investigation, Resources, Writing – original draft, Writing – review & editing, Visualization. **Ángela Baldrich:** Methodology, Software, Formal analysis, Investigation, Visualization. **Iván Pérez-Santos:** Conceptualization, Methodology, Formal analysis, Investigation, Resources, Writing – original draft, Writing – review & editing, Visualization. **Stephen J. Tomasetti:** Formal analysis, Investigation, Writing – original draft, Writing – review & editing. **Edwin Niklitschek:** Formal analysis, Investigation, Writing – original draft, Writing – review & editing. **Manuel Díaz:** Software, Formal analysis, Investigation, Visualization. **Gonzalo Álvarez:** Conceptualization, Methodology, Validation, Formal analysis, Investigation, Writing – original draft, Writing – review & editing. **Sandra L. Marín:** Software, Formal analysis, Investigation, Visualization. **Miriam Seguel:** Software, Formal analysis, Investigation, Visualization. **Laura Farías:** Conceptualization, Methodology, Validation, Formal analysis, Investigation, Visualization, Writing – review & editing, Funding acquisition. **Patricio A. Díaz:** Conceptualization, Methodology, Software, Validation, Formal analysis, Investigation, Resources, Writing – original draft, Writing – review & editing, Visualization, Supervision, Project administration, Funding acquisition.

Declaration of competing interest

The authors declare that they have no known competing financial interests or personal relationships that could have appeared to influence the work reported in this paper.

Acknowledgments

This work was funded by Comité Oceanográfico Nacional [CONA-C24F, 2018] by projects CONA C24F 18-06 (Patricio A. Díaz) and CONA 24F 18-07 (Laura Farías) and supported by REDI170575 from the International Cooperation Programme of the CONICYT. The authors also acknowledge the commander and crew of the AGS-61 "Cabo de Hornos" of the Chilean Navy for their support during the oceanographic campaign. The work of the Servicio Hidrográfico y Oceanográfico of Chilean Navy is also recognized. Laura Farías was funded by ANID by ICN2019_015 and FONDAP 1511009. We thank to Estrella Alcaman, Estrella Bello y Karen Sanzana for seawater sampling. Camilo Rodríguez-Villegas received a Ph.D. student fellowship from the Universidad de Los Lagos.

References

Agrawal, S., 2009. Factors affecting spore germination in algae. Folia Microbiol. 54, 273–302.

Álvarez, G., Díaz, P.A., Godoy, M., Araya, M., Ganuza, I., Pino, R., et al., 2019. Paralytic shellfish toxins in surf clams *Mesodesma donacium* during a large bloom of *Alexandrium catenella* Dinoflagellates associated to an intense shellfish mass mortality. Toxins 11, 188.

Amrhein, V., Greenland, S., McShane, B., 2019. Scientists Rise Up Against Statistical Significance. Nature Publishing Group.

Anderson, M.J., 2014. Permutational multivariate analysis of variance (PERMANOVA). Wiley statsref: statistics reference online 1–15.

Anderson, D.M., Chisholm, S.W., Waltras, C.J., 1983. Importance of life cycle events in the populations dynamics of *Gonyaulax tamarensis*. Mar. Biol. 76, 179–189.

Anderson, D.M., Taylor, C.D., Armbrust, E.V., 1987. The effects of darkness and anaerobiosis on dinoflagellate cyst germination1, 2. Limnol. Oceanogr. 32, 340–351.

Anderson, D.M., Keafer, B.A., McGillicuddy, D.J., Jr., Mickelson, M.J., Keay, K.E., Libby, P.S., et al., 2005. Initial observations of the 2005 *Alexandrium fundyense* bloom in southern New England: general patterns and mechanisms. Deep-Sea Res. II Top. Stud. Oceanogr. 52, 2856–2876.

Anderson, D.M., Burkholder, J.M., Cochlan, W.P., Glibert, P.M., Gobler, C.J., Heil, C.A., et al., 2008. Harmful algal blooms and eutrophication: examining linkages from selected coastal regions of the United States. Harmful Algae 8, 39–53.

Aracena, C., Lange, C.B., Iriarte, J.L., Rebolledo, L., Pantoja, S., 2011. Latitudinal patterns of export production recorded in surface sediments of the Chilean Patagonian fjords (41–55 S) as a response to water column productivity. Cont. Shelf Res. 31, 340–355.

Armijo, J., Oerder, V., Auger, P.-A., Bravo, A., Molina, E., 2020. The 2016 red tide crisis in southern Chile: possible influence of the mass oceanic dumping of dead salmons. Mar. Pollut. Bull. 150, 110603.

Azanza, R.V., Siringan, F.P., Diego-Mcglone, M.L.S., Yñiguez, A.T., Macalalad, N.H., Zamora, P.B., et al., 2004. Horizontal dinoflagellate cyst distribution, sediment characteristics and benthic flux in Manila Bay, Philippines. Phycol. Res. 52, 376–386.

Azanza, R.V., Brosnahan, M.L., Anderson, D.M., Hense, I., Montresor, M., 2018. The role of life cycle characteristics in harmful algal bloom dynamics. In: Global Ecology and Oceanography of Harmful Algal Blooms. Springer, pp. 133–161.

Band-Schmidt, C.J., Durán-Riveroll, L.M., Bustillos-Guzmán, J.J., Leyva-Valencia, I., López-Cortés, D.J., Núñez-Vázquez, E.J., et al., 2019. Paralytic toxin producing dinoflagellates in Latin America: ecology and physiology. Front. Mar. Sci. 6.

Binder, B.J., Anderson, D.M., 1987. Physiological and environmental control of germination in *Scrippsiella trochoidea* (Dinophyceae) resting cysts. J. Phycol. 23 (2), 99–107.

Boisnoir, A., Pavaux, A.-S., Schizas, N.V., Marro, S., Blasco, T., Lemée, R., et al., 2020. The use of stable isotopes to measure the ingestion rate of potentially toxic benthic dinoflagellates by harpacticoid copepods. J. Exp. Mar. Biol. Ecol. 524, 151285.

Bravo, I., Figueroa, R., 2014. Towards an ecological understanding of dinoflagellate cyst functions. Microorganisms 2, 11–32.

Brosnahan, M.L., Ralston, D.K., Fischer, A.D., Solow, A.R., Anderson, D.M., 2017. Bloom termination of the toxic dinoflagellate *Alexandrium catenella*: vertical migration behavior, sediment infiltration, and benthic cyst yield. Limnol. Oceanogr. 62, 2829–2849.

Brosnahan, M.L., Fischer, A.D., Lopez, C.B., Moore, S.K., Anderson, D.M., 2020. Cyst-forming dinoflagellates in a warming climate. Harmful Algae 91, 101728.

Burgess, R., 2001. An improved protocol for separating meiofauna from sediments using colloidal silica sols. Mar. Ecol. Prog. Ser. 214, 161–165.

A. Buschmann L. Farías F. Tapia D. Varela M. Vasquez Scientific report on the 2016 southern Chile red tide. Chilean Department of Economy www.academiadeficiencias.cl/wp-contentuploads201704infofinal_comisionmarearoja_21nov2016-pdf2016

Clarke, K.R., 1993. Non-parametric multivariate analyses of changes in community structure. Aust. J. Ecol. 18, 117–143.

Clarke, K., Warwick, R., 1994. An approach to statistical analysis and interpretation. Change Mar. Commun. 2, 117–143.

Crawley, M., 2007. The R Book. John Wiley & Sons, Chichester, UK.

Dale, B., 1976. Cyst formation, sedimentation, and preservation: factors affecting dinoflagellate assemblages in recent sediments from Trondheims fjord, Norway. Rev. Palaeobot. Palynol. 22, 39–60.

Dale, B., 1983. Dinoflagellate resting cysts: "benthic plankton". In: Survival Strategies of the Algae. pp. 69–136.

Dale, A.L., Dale, B., 1992. Dinoflagellate contributions to the sediment flux of the Nordic seas. Ocean Biocoenosis Ser. 5, 45–76.

De Camargo, M.G., 2016. SysGran: um sistema de código aberto para análises granulométricas do sedimento. Revista Brasileira de Geociências 36, 371–378.

De Troch, M., Vergaerde, I., Cnudde, C., Vanormelingen, P., Vyverman, W., Vincx, M., 2012. The taste of diatoms: the role of diatom growth phase characteristics and associated bacteria for benthic copepod grazing. Aquat. Microb. Ecol. 67, 47–58.

Díaz, P., Molinet, C., Seguel, M., Dıaz, M., Labra, G., Figueroa, R.I., 2014. Coupling planktonic and benthic shifts during a bloom of *Alexandrium catenella* in southern Chile: implications for bloom dynamic and recurrence. Harmful Algae 40, 9–22.

Díaz, P.A., Molinet, C., Seguel, M., Díaz, M., Labra, G., Figueroa, R.I., 2018. Species diversity and abundance of dinoflagellate resting cysts seven months after a bloom of *Alexandrium catenella* in two contrasting coastal systems of the Chilean Inland Sea. Eur. J. Phycol. 53, 410–421.

Díaz, P.A., Álvarez, A., Varela, D., Pérez-Santos, I., Díaz, M., Molinet, C., et al., 2019. Impacts of harmful algal blooms on the aquaculture industry: Chile as a case study. Perspect. Phycol..

Ellegaard, M., Ribeiro, S., 2018. The long-term persistence of phytoplankton resting stages in aquatic 'seed banks'. Biol. Rev. 93, 166–183.

Fertouna-Bellakhal, M., Dhib, A., Béjaoui, B., Turki, S., Aleya, L., 2014. Driving factors behind the distribution of dinocyst composition and abundance in surface sediments in a western Mediterranean coastal lagoon: report from a high resolution mapping study. Mar. Pollut. Bull. 84, 347–362.

Figueroa, R.I., Bravo, I., Garcés, E., 2005. Effects of nutritional factors and different parental crosses on the encystment and excystment of *Alexandrium catenella* (Dinophyceae) in culture. Phycologia 44 (6), 658–670.

Figueroa, R.I., Garces, E., Bravo, I., 2007. Comparative study of the life cycles of *Alexandrium tamutum* and *Alexandrium minutum* (Gonyaulacales, Dinophyceae) in culture 1. J. Phycol. 43, 1039–1053.

Figueroa, R.I., Estrada, M., Garcés, E., 2018. Life histories of microalgal species causing harmful blooms: haploids, diploids and the relevance of benthic stages. Harmful Algae 73, 44–57.

Fischer, A.D., Brosnahan, M.L., Anderson, D.M., 2018. Quantitative response of *Alexandrium catenella* cyst dormancy to cold exposure. Protist 169, 645–661.

Fox, J., Weisberg, S., 2011. An R Companion to Applied Regression. 2nd ed. Sage Publications, California, USA.

Franco, M., Soetaert, K., Costa, M., Vincx, M., Vanaverbeke, J., 2008. Uptake of phytodetritus by meiobenthos using 13C labelled diatoms and *Phaeocystis* in two contrasting sediments from the North Sea. J. Exp. Mar. Biol. Ecol. 362, 1–8.

Fryxell, G.A., 1983. Survival Strategies of the Algae. CUP Archive.

Genovesi, B., Laabir, M., Masseret, E., Collos, Y., Vaquer, A., Grzebyk, D., 2009. Dormancy and germination features in resting cysts of *Alexandrium tamarense* species

complex (Dinophyceae) can facilitate bloom formation in a shallow lagoon (Thau, southern France). J. Plankton Res. 31, 1209–1224.
Genovesi-Giunti, B., Laabir, M., Vaquer, A., 2006. The benthic resting cyst: a key actor in harmful dinoflagellate blooms-a review. Vie et milieu 56, 327–337.
Giere, O., 2009. Meiobenthology: The Microscopic Motile Fauna of Aquatic Sediments. Springer Science & Business Media.
Godhe, A., Sjöqvist, C., Sildever, S., Sefbom, J., Harðardóttir, S., Bertos-Fortis, M., et al., 2016. Physical barriers and environmental gradients cause spatial and temporal genetic differentiation of an extensive algal bloom. J. Biogeogr. 43, 1130–1142.
Gotelli, N.J., Ellison, A.M., 2004. Primer of Ecological Statistics. Sinauer Associates Publishers.
Grasshoff, K., Ehrhardt, M., Kremling, K., 1983. Methods of seawater analysis. Chemie. Weinheim.
Grego, M., Riedel, B., Stachowitsch, M., De Troch, M., 2014. Meiofauna winners and losers of coastal hypoxia: case study harpacticoid copepods. Biogeosciences 11, 281–292.
Guiry, M.D., 2020. In: Guiry, M.D., Guiry, G.M. (Eds.), World-Wide Electronic Publication. National University of Ireland, Galway AlgaeBase http://www.algaebase.org; (searched on 17 August. 2020).
Guzmán, L., Campodónico, I., Antunovic, M., 1975. Estudios sobre un florecimiento tóxico causado por *Gonyaulax catenella* en Magallanes. In: IV. Distribución y niveles de toxicidad del Veneno Paralítico de los Mariscos (noviembre de 1972-noviembre de 1973). Anales del Instituto de la Patagonia.
Guzmán L, Pacheco H, Pizarro G, Alárcon C. *Alexandrium catenella* y veneno paralizante de los mariscos en Chile. In: Sar, E. A., Ferrario, M. E., Reguera, B. (Eds.). Floraciones Algales Nocivas en el Cono Sur Americano. Instituto Español de Oceanografía, Madrid 2002: 235–255.
Hallegraeff, G.M., 1993. A review of harmful algal blooms and their apparent global increase. Phycologia 32, 79–99.
Hallegraeff, G.M., 2010. Ocean climate change, phytoplankton community responses, and harmful algal blooms: a formidable predictive challenge 1. J. Phycol. 46, 220–235.
Hernández, C., Díaz, P.A., Molinet, C., Seguel, M., 2016. Exceptional climate anomalies and north wards expansion of paralytic shellfish poisoning outbreaks in southern Chile. Harmful algae News 54, 1–2.
Holmes, R.M., Aminot, A., Kérouel, R., Hooker, B.A., Peterson, B.J., 1999. A simple and precise method for measuring ammonium in marine and freshwater ecosystems. Can. J. Fish. Aquat. Sci. 56, 1801–1808.
Horner, R., Greengrove, C.L., Davies-Vollum, K., Gawel, J.E., Postel, J., Cox, A., 2011. Spatial distribution of benthic cysts of *Alexandrium catenella* in surface sediments of Puget Sound, Washington, USA. Harmful Algae 11, 96–105.
Iriarte, J.L., Pantoja, S., Daneri, G., 2014. Oceanographic processes in Chilean fjords of Patagonia: from small to large-scale studies. Prog. Oceanogr. 129, 1–7.
Kremp, A., Anderson, D.M., 2000. Factors regulating germination of resting cysts of the spring bloom dinoflagellate *Scrippsiella hangoei* from the northern Baltic Sea. J. Plankton Res. 22, 1311–1327.
Kremp, A., Oja, J., LeTortorec, A.H., Hakanen, P., Tahvanainen, P., Tuimala, J., et al., 2016. Diverse seed banks favour adaptation of microalgal populations to future climate conditions. Environ. Microbiol. 18, 679–691.
Kremp, A., Hinners, J., Klais, R., Leppänen, A.-P., Kallio, A., 2018. Patterns of vertical cyst distribution and survival in 100-year-old sediment archives of three spring dinoflagellate species from the Northern Baltic Sea. Eur. J. Phycol. 53, 135–145.
Lee, M.R., Torres, R., Manríquez, P.H., 2017. The combined effects of ocean warming and acidification on shallow-water meiofaunal assemblages. Mar. Environ. Res. 131, 1–9.
Legendre, P., Legendre, L., 1998. Numerical ecology. 2nd English edition Elsevier, Amsterdam, The Netherlands.
Mardones, J.I., Bolch, C., Guzmán, L., Paredes, J., Varela, D., Hallegraeff, G.M., 2016. Role of resting cysts in Chilean *Alexandrium catenella* dinoflagellate blooms revisited. Harmful Algae 55, 238–249.
Marret, F., Zonneveld, K.A., 2003. Atlas of modern organic-walled dinoflagellate cyst distribution. Rev. Palaeobot. Palynol. 125, 1–200.
Matsuoka, K., 1999. Eutrophication process recorded in dinoflagellate cyst assemblages—a case of Yokohama Port, Tokyo Bay, Japan. Sci. Total Environ. 231, 17–35.
Matsuoka, K., Fukuyo, Y., 2000. Technical Guide for Modern Dinoflagellate Cyst Study. WESTPAC-HAB, Japan Society for the Promotion of Science, Tokyo, Japan, pp. 6–9.
McCullagh, P., Nelder, J., 1989. Generalized linear models. In: Standard Book on Generalized Linear Models, 2nd edn Chapman and Hall, London.
McGillicuddy, D., Jr., Townsend, D.W., He, R., Keafer, B.A., Kleindinst, J.L., Li, Y., et al., 2011. Suppression of the 2010 *Alexandrium fundyense* bloom by changes in physical, biological, and chemical properties of the Gulf of Maine. Limnol. Oceanogr. 56, 2411–2426.
Molinet, C., Lafon, A., Lembeye, G., Moreno, C.A., 2003. Patrones de distribución espacial y temporal de floraciones de *Alexandrium catenella* (Whedon & Kofoid) Balech 1985, en aguas interiores de la Patagonia noroccidental de Chile. Rev. Chil. Hist. Nat. 76, 681–698.
Montresor, M., Marino, D., 1996. Modulating effect of cold-dark storage on excystment in *Alexandrium pseudogonyaulax* (Dinophyceae). Mar. Biol. 127, 55–60.
Mudie, P., Rochon, A., Aksu, A., Gillespie, H., 2002. Dinofagellate cysts, freshwater algae and fungal spores as salinity indicators in late quaternary cores from Marmara and Black seas. Mar. Geol. 19, 203–231.
Nehring, S., 1993. Mechanisms for Recurrent Nuisance Algal Blooms in Coastal Zones: Resting Cyst Formation as Life-Strategy of Dinoflagellates. Lang.
Oksanen J, Blanchet F, Kindt R, Legendre P, Minchin P, O'Hara R, et al. Package 'vegan'—community ecology package. 2019. View Article 2018.
Olli, K., Trunov, K., 2010. Abundance and distribution of vernal bloom dinoflagellate cysts in the Gulf of Finland and Gulf of Riga (the Baltic Sea). Deep-Sea Res. II Top. Stud. Oceanogr. 57, 235–242.
Paliy, O., Shankar, V., 2016. Application of multivariate statistical techniques in microbial ecology. Mol. Ecol. 25, 1032–1057.
Paredes-Mella, J., Varela, D., Fernández, P., Espinoza-González, O., 2020. Growth performance of *Alexandrium catenella* from the Chilean fjords under different environmental drivers: plasticity as a response to a highly variable environment. J. Plankton Res. 42, 119–134.
Pati, A., Belmonte, G., Ceccherelli, V., Boero, F., 1999. The inactive temporary component: an unexplored fraction of meiobenthos. Mar. Biol. 134, 419–427.
Pérez-Santos I, Garcés-Vargas J, Schneider W, Ross L, Parra S, Valle-Levinson A. Double-diffusive layering and mixing in Patagonian fjords. Prog. Oceanogr. 2014; 129: 35–49.
Persson, A., 2000. Possible predation of cysts—a gap in the knowledge of dinoflagellate ecology? J. Plankton Res. 22, 803–809.
Pfannkuche, O., Thiel, H., 1988. Sample processing. In: Introduction to the Study of Meiofauna, 9. pp. 134–145.
Price, A.M., Pospelova, V., Coffin, M.R.S., Latimer, J.S., Chmura, G.L., 2016. Biogeography of dinoflagellates in northwest Atlantic estuaries. Ecol. Evol. 6, 5648–5662.
R Core Team. R: A language and environment for statistical computing. R foundation for statistical computing, Vienna, Austria. URL https://www.R-project.org/. 2019.
Rengefors, K., Anderson, D.M., 2002. Environmental and endogenous regulation of cyst germination in two freshwater dinoflagellates. J. Phycol. 34, 568–577.
Rengefors, K., Anderson, D.M., Pettersson, K., 1996. Phosphorus uptake by resting cysts of the marine dinoflagellate Scrippsiella trochoidea. J. Plankton Res. 18 (9), 1753–1765.
Ribeiro, S., Berge, T., Lundholm, N., Andersen, T.J., Abrantes, F., Ellegaard, M., 2011. Phytoplankton growth after a century of dormancy illuminates past resilience to catastrophic darkness. Nat. Commun. 2, 311.
Ribeiro, S., Berge, T., Lundholm, N., Ellegaard, M., 2013. Hundred years of environmental change and phytoplankton ecophysiological variability archived in coastal sediments. PLoS One 8, e61184.
Rodríguez-Villegas, C., Díaz, P.A., Pizarro, G., Salgado, P., Pérez-Santos, I., Díaz, M., et al., 2020. *Alexandrium catenella* cyst accumulation by passive and active dispersal agents: implications for the potential spreading risk in Chilean Patagonian fjords. Harmful Algae 96.
Sætre, M.M., Dale, B., Abdullah, M.I., Sætre, G.-P., 1997. Dinoflagellate cysts as potential indicators of industrial pollution in a Norwegian fjord. Mar. Environ. Res. 44, 167–189.
SalmonChile. Production data. 2018.
R. Schlitzer Ocean data view https://odv.awi.de2019
Sernapesca, 2017. Anuario estadístico de pesca. Servicio Nacional de Pesca. Valparaíso.
Sievers H, Silva N. Water masses and circulation in austral Chilean channels and fjords. Progress in the oceanographic knowledge of Chilean interior waters, from Puerto Montt to Cape Horn 2008: 53–58.
Silva, N., Calvete, C., 2002. Caracteristicas oceanograficas fisicas y quimicas de canales australes chilenos entre el golfo de Penas y el estrecho de Magallanes (Crucero CIMAR-Fiordo 2). Revista Ciencia y Tecnología del Mar 25, 1.
Silva, N., Palma, S., 2006. Características físicas y químicas de los sedimentos superficiales de canales y fiordos australes. In: Avances En El Conocimiento Oceanográfico de Las Aguas Interiores Chilenas, Puerto Montt a Cabo de Hornos. CONA e PUCV. pp. 69–75.
Silva, N., Vargas, C.A., 2014. Hypoxia in Chilean patagonian fjords. Prog. Oceanogr. 129, 62–74.
Silva N, Sievers H, Prado R. Características oceanográficas y una proposición de circulación, para algunos canales australes de Chile entre 41° 20'S y 46° 40'S. Rev. Biol. Mar 1995; 30: 207–254.
Torres, R., Silva, N., Reid, B., Frangopulos, M., 2014. Silicic acid enrichment of subantartic surface water from continental inputs along the Patagonian archipielago interior sea (41–56°S). Prog. Oceanogr. 129, 50–61.
Tubaro, A., Dell'Ovo, V., Sosa, S., Florio, C., 2010. Yessotoxins: a toxicological overview. Toxicon 56, 163–172.
Varela, D., Paredes, J., Alves-de-Souza, C., Seguel, M., Sfeir, A., Frangópulos, M., 2012. Intraregional variation among *Alexandrium catenella* (Dinophyceae) strains from southern Chile: morphological, toxicological and genetic diversity. Harmful Algae 15, 8–18.
Venables, W.N., Ripley, B.D., 2010. Modern Applied Statistics with S. Springer Publishing Company, Incorporated.
Venables, W.N., Ripley, B.D., 2013. Modern Applied Statistics with S-PLUS. Springer Science & Business Media.
Wasserstein, R.L., Lazar, N.A., 2016. The ASA Statement on P-Values: Context, Process, and Purpose. Taylor & Francis.
Wentworth, C.K., 1922. A scale of grade and class terms for clastic sediments. J. Geol. 30, 377–392.
Xu, Y., Zhang, T., Zhou, J., 2019. Historical occurrence of algal blooms in the northern Beibu Gulf of China and implications for future trends. Front. Microbiol. 10, 451.
Zonneveld, K.A., Marret, F., Versteegh, G.J., Bogus, K., Bonnet, S., Bouimetarhan, I., et al., 2013. Atlas of modern dinoflagellate cyst distribution based on 2405 data points. Rev. Palaeobot. Palynol. 191, 1–197.